Zoologischer Anzeiger
Article In Press
Acceptation date : June 2019
https://doi.org/10.1016/j.jcz.2019.05.007
https://archimer.ifremer.fr/doc/00502/61330/

Archimer
https://archimer.ifremer.fr

Deep-sea Kinorhyncha diversity of the polymetallic nodule fields at the Clarion-Clipperton Fracture Zone (CCZ)

Sánchez Nuria [1, 2, *], Pardos Fernando [1], Arbizu Pedro Martínez [3]

[1] Department of Zoology and Anthropology, Universidad Complutense de Madrid, Madrid, Spain
[2] IFREMER, Centre Brest, REM/EEP/LEP, ZI de la pointe du diable, CS10070, 29280, Plouzané, France
[3] Deutsches Zentrum für Marine Biodiversitätsforschung, Senckenberg am Meer, Germany

* Corresponding author : Nuria Sánchez, email address : nurisanc@ucm.es

Abstract :

Kinorhynch specimens were studied from abyssal sediment samples collected during seven cruises at the Clarion-Clipperton Fracture Zone (Eastern Central Pacific), a vast area that will be mined for polymetallic nodules in a near future. This study is the first in a series focused on kinorhynchs mainly collected at the German zone following requirements of the International Seabed Authority (ISA), who demands identification of fauna associated with nodules previous to the concession of the exploitation license. A total of 18 species were found, of which three new Echinoderidae species are described herein. *Cephalorhyncha polunga* sp. nov. is easily discriminated from its congeners by the presence of pointed and prominent tergal extensions together with middorsal spines on segments 4-8, ventrolateral tubes on segment 2, lateroventral tubes on segment 5, lateroventral spines on segments 6–9 and midlateral tubes on segment 10; plus subdorsal type 2 glandular cell outlets on segment 2 and midlateral ones on segment 8. *Echinoderes shenlong* sp. nov. is characterized by middorsal spines on segments 4, 6, 8, lateroventral tubes on segment 5 and lateroventral spines on segments 6-9; glandular cell outlets type 2 are not present. *Meristoderes taro* sp. nov. is defined by the combination of long middorsal spines on segments 4-8, remarkably increasing in length on posterior segments; short laterodorsal tubes on segment 10, ventrolateral tubes on segment 2 and lateroventral tubes on segment 5, plus lateroventral spines on segments 6-9.

Keywords : *Cephalorhyncha*, Cyclorhagida, Echinoderidae, Echinoderes, meiofauna, *Meristoderes*, taxonomy

Please note that this is an author-produced PDF of an article accepted for publication following peer review. The definitive publisher-authenticated version is available on the publisher Web site.

1. Introduction

Polymetallic nodule areas of the seabed are currently in the spotlight due to their potential commercial and strategic interest related to the presence of metals such as nickel, copper, cobalt and rare earth elements, which make up the black spheroidal/discoidal bodies commonly referred as manganese nodules (Halbach et al., 1975; Halbach and Fellerer, 1980). The polymetallic nodule fields occur in deep-sea bottoms with low sedimentation rates, where nodules lie on the soft sediment increasing the heterogeneity of the environment and hence its biodiversity compared to that of typical abyssal areas (Amon et al., 2016; de Smet et al., 2017; Janssen et al., 2015; Kaiser et al., 2017; Ramirez-Llodra et al., 2010; Smith et al., 2008; Vanreusel et al., 2016). The nodules harbour organisms inhabiting the sediment of the nodule crevices, or sessile communities dependent of hard substrates (Amon et al., 2016; Thiel et al., 1993; Vanreusel et al., 2016; Veillette et al., 2007). Even though it is expected that nodules will be mined in the near future in order to face the growing demand of valuable metals (Clark et al., 2013), the biological diversity of the nodule fields is still poorly known, even for the macrofauna realm (Amon et al., 2016; Glover et al., 2002; Janssen et al., 2015; Paterson et al., 1998; Smith et al., 2008). Thus, the International Seabed Authority (ISA) requires identification of the associated fauna with the nodule areas before the concession of the exploitation, in order to assess accurate environmental impact predictions and to establish mining regulations (ISA-LTC, 2013). These tasks are crucial for biodiversity since mining operations may cause severe disturbances in the environment, not only because of the extraction of the nodules themselves, which decreases heterogeneity and directly affects fauna dependent on nodules for habitat (biodiversity loss), but also because it will impact the biota of the soft sediments by compression of top layers and resuspension of particles (Vanreusel et al., 2016).

Regarding the meiofauna diversity, most of the studies have focused on the dominant groups, such as Nematoda and Copepoda (Markhaseva et al., 2017; Miljutin et al., 2011; Singh et al., 2016), whereas the groups of low abundance, the so-called “minor phyla”, have been neglected so far. Kinorhyncha, free-living marine ecdysozoan of small size (0.1-1 mm) exclusively meiobenthic, belongs to this pool of “minor phyla”. Despite kinorhynchs, or mud dragons, appear worldwide, from the intertidal to the

deep-sea bottoms, most of the nearly 300 described species were recorded at relatively shallow waters whilst the deep-sea kinorhynch fauna is still largely unexplored.

Our study is the first to focus on Kinorhyncha from the polymetallic nodule fields of the greatest commercial interest, the Clarion-Clipperton Fracture Zone (CCZ) (northeastern equatorial Pacific Ocean), mainly at the German Federal Institute for Geosciences and Natural Resources (BGR) license area and nearby areas. This manuscript is the first in a series with the main aim of filling the knowledge gap of deep-sea "minor phyla" diversity in general, and particularly of the kinorhynch diversity at the CCZ. Moreover, these studies will lead to assess how animals may be affected by seafloor mining activities, and help in the selection of effective preservation of areas.

2. Materials and methods

Kinorhynch specimens were obtained from deep-sea sediment samples from the German license area (German Federal Institute for Geoscience and Natural Resources, BGR) at the Clarion-Clipperton Fracture Zone (NE Pacific Ocean), collected during 7 cruises that lasted from 2010 to 2016: MANGAN 2010 (R/V Sonne), MANGAN 2014 (R/V Kilo Moana), MANGAN 2016 (R/V Kilo Moana), FLUM (R/V Sonne), JPIO/CCZ (R/V Sonne), JPIO/DISCOL (R/V Sonne), ABYSSLINE II (R/V Thomas G. Thompson) (some samples collected during the referred samples campaigns at nearby areas belonging to other contractors and at the Peru Basin were also studied). Samples were collected at abyssal depths between 4090 and 5012 m using a multicorer with corers of 9.4 cm of inner diameter sampling a total surface area of 69 cm^2 by each core (see Table 1 for detailed information of each sample).

The upper 5 cm of the soft sediment from each core was fixed in 4% buffered formalin. Samples were then washed in the laboratory at the Senckenberg Research Institute in Wilhelmshaven, Germany, and meiofauna was extracted from the sediment through centrifugation with the colloidal silica polymer Levasil (Neuhaus and Blasche, 2006). Subsequently, the extracted meiofauna was sorted to main groups. Cores with nodules were treated by carefully removing the nodules, which were subsequently washed, and sediment from the nodule surface and crevices was collected. This sediment was fixed in 4% buffered formalin, washed at the laboratory and meiofauna was sorted to main

groups. A total of 723 kinorhynchs from 272 cores were sorted and stored in 70% ethanol.

Specimens for light microscopic (LM) observation were dehydrated through a graded series of glycerin and kept overnight in 100% glycerin. Then the specimens were mounted in Fluoromount-G® on glass slides, examined and photographed with an Olympus BX51 compound microscope with differential interference contrast (DIC) optics equipped with an Olympus DP70 camera. Specimens were measured with cellSens® software. Line art figures were made with Adobe Illustrator CS6 software.

Additionally, specimens for scanning electron microscopy (SEM) were dehydrated through a series of 80%, 90%, 95% and 100% ethanol, and chemically dried using Hexamethyldisilazane (HMDS) through HMDS-ethanol series. Finally, they were mounted on a SEM stub, sputter coated with gold, and examined with a JEOL JSM-6335F field mission scanning electron microscope at the ICTS Centro Nacional de Microscopía Electrónica (Complutense University of Madrid, Spain).

The type and additional material of the new species is deposited at the Museum für Naturkunde (MfN), Humboldt-Universität zu Berlin, Germany.

3. Results

Taxonomic account

Class Cyclorhagida (Zelinka, 1896) *sensu* Sørensen et al., 2015

Order Echinorhagata Sørensen et al., 2015

Family Echinoderidae Zelinka, 1894

Genus *Cephalorhyncha* Adrianov, 1999 in Adrianov and Malakhov (1999)

3.1. *Cephalorhyncha polunga* sp. nov.

(Figs. 2-4)

ZooBank lsid: urn: lsid:zoobank.org:act:104DD93C-791C-4366-9A52-7DFAECBDE2EA

3.1.1. Examined material

Holotype, adult male, collected on June 8, 2015, Flum cruise, station MUC #109, North Pacific: 11°48.791' N, 116°31.76' W, at 4327 m depth in soft sediment; mounted in Fluoromount G®, deposited at MfN under accession number: ZMB XXXXX. 9 paratypes, 5 adult females and 4 adult males, all of them collected at other stations than holotype (see Table 1), mounted in Fluoromount G® and stored at MfN under accession numbers: ZMBXXXXX–XXXXX. One specimen mounted for SEM and 13 additional specimens mounted for LM are deposited at the MfN as additional material.

3.1.2. Diagnosis

Cephalorhyncha with middorsal spines on segments 4-8, increasing in length on posterior segments; ventrolateral tubes and subdorsal glandular cell outlets type 2 on segment 2; lateroventral tubes on segment 5 and lateroventral spines on segments 6–9; midlateral type 2 glandular cell outlets on segment 8; midlateral tubes on segment 10. Prominent tergal extensions, distally pointed.

3.1.3. Etymology

The species name refers to Polunga, the most powerful and biggest dragon of the manga and anime “Dragon Ball” by Akira Toriyama. Polunga is a wish granting dragon summoned when all seven spherical magic balls, Earth's Dragon Balls, are gathered together and symbolizes the relationship between mud dragons and nodules reported herein.

3.1.4. Description

All dimensions and measurements are summarized in Table 2, and distribution of cuticular structures in Table 3.

Head and neck. Mouth cone with 9 outer oral styles alternating in size between slightly longer and shorter ones, and consisting of two jointed subunits. Introvert with several rings of cuticular spinoscalids whose exact number, arrangement and detailed morphology could not be determined with LM. One additional ring of trichoscalids present, composed of six long trichoscalids attached to small trichoscalid plates. The neck consists of 16 trapezoidal placids, with wider bases, distinctly articulating with

segment 1 (Fig. 3A-B). Midventral placid broader than the remaining ones (ca. 15 μm wide at base), while the remaining ones are of similar size (ca. 9 μm wide at base) (Fig. 3C). Placids separated by cuticular folds at the distal end.

Trunk. 11 segments, with segment 1 formed by a closed cuticular ring, segment 2 by one tergal and one sternal plate, partially divided midventrally, and remaining ones by one tergal and two sternal cuticular plates (Figs. 2A-B, 3A-B and 4A-B). Midsternal junctions well-developed on segments 3 to 11, and tergosternal junctions on segments 2 to 11. Sternal plates reach their maximum width at segment 7, progressively tapering towards the last trunk segments. General outline of the trunk slender. Cuticular hairs long, filiform, bracteate (Fig. 4F) and arranged in three main wavy transverse rows until almost half of the sternal plates, with the hairs of the anterior row surpassing the insertion of the following one, and with those of the last row reaching the pectinate fringe area (Fig. 4D-E). Sensory spots composed of a single pore surrounded by few, short micropapillae (Fig. 4D) that can be flanked by two non-bracteate cuticular hairs on segment 1. Posterior segment margin straight, showing well-developed primary pectinate fringes with elongated, strongly serrated free flap (Figs. 3C, H, J and 4G).

Segment 1 as a closed cuticular ring (Fig. 3C), lacking spines or tubes. Cuticular hairs on this segment are equally distributed along the plate, less abundant than on the following ones. Pectinate fringe less developed than on following segments (Fig. 3C). An unpaired type 1 glandular cell outlet present in middorsal position, and paired ones in lateroventral and ventrolateral positions; paired sensory spots in subdorsal and laterodorsal positions (Figs. 2A, B and 3C).

Segment 2 with one tergal and one sternal plate; sternal plate partially divided into two ventral plates by midsternal incomplete, intracuticular fissure (Figs. 2A and 3C-D). A single middorsal type 1 glandular cell outlet and sensory spot (Fig. 4D), paired type 2 glandular cell outlets in subdorsal position (Fig. 3E), one pair of laterodorsal and midlateral sensory spots (Fig. 3E, G). Paired long, thick tubes located in ventrolateral position (Fig. 3C), and ventromedial pair of sensory spots and type 1 glandular cell outlets present (Fig. 3C). Cuticular hairs mostly absent at the area next to the midventral line.

Segment 3 with unpaired middorsal type 1 glandular cell outlet, paired subdorsal sensory spots (Figs. 3G and 4D) and ventromedial type 1 glandular cell outlet (Fig. 3C).

Cuticular hairs ventrally arranged in patches covering the lateral half of the plates (Fig. 3C).

Segment 4 with a middorsal acicular spine exceeding the posterior edge of the segment, reaching half of the following dorsal plate (Fig. 3A, G). Paired type 1 glandular cell outlets in paradorsal and ventromedial positions (Fig. 2A-B). Pattern of cuticular hairs at the dorsal side with hairless longitudinal bands in middorsal and laterodorsal positions. Ventral cuticular hairs arranged as in the preceding segment.

Segment 5 similar to segment 4 but with longer middorsal acicular spine (Figs. 3A, H and 4C), plus one pair of laterodorsal sensory spots (Fig. 3G) and lateroventral tubes (Fig. 2A). Otherwise similar to preceding segment.

Segment 6 with a middorsal acicular spine longer than that of the preceding segment, exceeding the posterior margin of the following segment (Figs. 3A, H and 4A, C, G). Paired paradorsal type 1 glandular cell outlets at the anterior dorsal margin (Fig. 2B). One pair of sensory spots in paradorsal position, flanking the middorsal spine and located posterior to its base (Figs. 3H, 4G). One pair of small midlateral sensory spots (Fig. 2B), lateroventral acicular spines that reach half of the following segment (Fig. 3E, J) and ventromedial type 1 glandular cell outlets. Otherwise similar to preceding segment.

Segment 7 with cuticular structures on tergal and sternal plates similar to those of segment 6 but with a longer middorsal spine reaching segment 9 (Figs. 3A, H and 4A, C, F-G), without midlateral sensory spots and with paired and sensory spots in ventromedial position (Fig. 3J).

Segment 8 with cuticular structures on tergal and sternal plates similar to those of segment 6 but with much longer spines (Figs. 3A, H-I and 4A, C, F), and with paired type 2 glandular cell outlets in midlateral position (Figs. 3E, I and 4F, I) instead of sensory spots. The middorsal spine surpasses the posterior margin of the last trunk segment (Figs. 3A and 4A), and the lateroventral ones reach at least the posterior margin of segment 9 (Fig. 3B, J).

Segment 9 without middorsal spine (Fig. 3H-I) and with pairs of long lateroventral acicular spines reach the terminal trunk segment (Fig. 3B). Pairs of paradorsal type 1 glandular cell outlets and sensory spots, plus paired sensory spots in

subdorsal, laterodorsal (Figs. 3H-I and 4F) and ventrolateral positions (Fig. 3K), and paired ventromedial type 1 glandular cell outlets. Paradorsal and subdorsal sensory spots located near the middle of the plate, and the laterodorsal pair appears posteriorly located, closer to the pectinate fringe (Fig. 3H-I). Nephridiopore as a small sieve plate present in sublateral position (Fig. 3K). Middorsal and laterodorsal hairless areas along the whole longitudinal line of the plate. Otherwise similar to preceding segment.

Segment 10 with two unpaired, longitudinally aligned middorsal type 1 glandular cell outlets, plus one pair of paradorsal sensory spots, long midlateral tubes in both sexes (Fig. 3F, I), ventrolateral sensory spots and ventromedial type 1 glandular cell outlets (Fig. 2A). Posterior ventral segment margin deeply curved, extending posteriorly in the ventromedial area (Fig. 3F). Otherwise similar to preceding segment.

Segment 11 with long lateral terminal spines and distally pointed tergal extensions (Figs. 3F and 4H). Tergal plate with one pair of subdorsal sensory spots (Fig. 3I) and a middorsal protuberance protruding from the intersegmental joint between segments 10 and 11 (Figs. 2B, D, 3I and 4H). Sternal plates with one pair of ventrolateral sensory spots. Cuticular hairs less abundant at both dorsal and ventral sides. Females with one pair of thick and long lateral terminal accessory spines (Figs. 3F and 4H), about one third of length of lateral terminal spines. Males with three pairs of penile spines; ventral and dorsal penile spines filiform, midlateral penile spine shorter and coarser.

Associated kinorhynch fauna. Fissuroderes higginsi Neuhaus and Blasche, 2006; *Campyloderes vanhöffeni* Zelinka, 1913; *Semnoderes pacificus* Higgins, 1967; *Echinoderes shenlong* sp. nov., *Meristoderes taro* sp. nov., *Echinoderes* sp. 1, *Echinoderes* sp. 2 and *Echinoderes* sp. 4.

3.1.5. Remarks

The presence of elongated middorsal spines on segments 4 to 8, increasing in length towards the posterior segments is shared with most other species of *Cephalorhyncha*: *Cephalorhyncha asiatica* (Adrianov, 1989), *Cephalorhyncha flosculosa* Yildiz, Sørensen and Karaytuğ, 2016, *Cephalorhyncha liticola* Sørensen, 2008, and *Cephalorhyncha nybakkeni* (Higgins, 1986), (Adrianov, 1989; Higgins, 1986; Sørensen,

2008; Yildiz et al., 2016). Only a newly described species of *Cephalorhyncha* (see Cepeda et al., this issue) differs from this pattern, bearing middorsal spines only on segments 4, 6 and 8 plus sublateral spines on segment 7.

However, three congeners, *C. asiatica*, *C. liticola*, and *C. flosculosa*, with middorsal spines on segments 4 to 8 have lateral accessory tubes or spines on segment 8 whereas the new species lacks any cuticular appendage in lateral accessory position. Likewise, none of these species have type 2 glandular cell outlets, which are present and easily detectable subdorsally on segment 2 and midlaterally on segment 8 in *Cephalorhyncha polunga* sp. nov.

The single *Cephalorhyncha* species described so far lacking tubes/spines in sublateral or lateral accessory positions is *C. nybakkeni* (Higgins, 1986). This species furthermore differs from *C. polunga* sp. nov. by having shorter tergal extensions, shorter middorsal spines on segments 6-7, no glandular cell outlets type 2, plus short and robust lateral terminal accessory spines in females (Higgins, 1986).

3.2. Genus *Echinoderes* Claparède, 1863

***Echinoderes shenlong* sp. nov.**

(Figs. 5-7)

ZooBank lsid: urn: lsid:zoobank.org:act:41A5B46C-0158-4F60-827C-36F06959EDC5.

3.2.1 Examined material

Holotype, adult female, collected on May 18, 2015, Flum cruise, station MUC #37, North Pacific: 12°54.131' N, 118°24.782' W at 4319 m depth in soft sediment; mounted in Fluoromount G®, deposited at MfN under accession number: ZMB XXXXX. 4 paratypes, 3 adult females and 1 adult male (see Table 1 for further information on stations), mounted in Fluoromount G® and deposited at the MfN under accession numbers: ZMB XXXXX–XXXXX. One additional female specimen mounted for SEM, deposited at the MfN as additional material.

3.2.2 Diagnosis

Echinoderes with middorsal spines on segments 4, 6, 8, increasing in length on posterior segments; lateroventral tubes on segment 5 and lateroventral spines on segments 6-9. Glandular cell outlets type 2 absent. Tergal extensions, broadly rounded and spatulate.

3.2.3. Etymology

The species name refers to Shenlong, one of the dragons of the manga and anime "Dragon Ball" by Akira Toriyama, also known as the Eternal Dragon in the Ocean. Shenlong is a wish granting dragon summoned when all seven spherical magic balls, Earth's Dragon Balls, are gathered together.

3.2.4. Description

All dimensions and measurements are summarized in Table 4, and distribution of cuticular structures in Table 5.

Head and neck. Arrangement and detailed morphology of the head could not be determined as none of the studied specimens were suitable for introvert examinations. The neck consists of 16 trapezoidal placids, with wider bases (Figs. 6A-B, F and 7A-B). All placids of similar size and shape (ca. 6 μm wide at base), except for the broader midventral one (ca. 10 μm wide at base). Placids distally separated by cuticular folds. Six trichoscalid plates attached to the placids.

Trunk. 11 segments, with segments 1 and 2 formed by a closed cuticular ring, and remaining ones by one tergal and two sternal cuticular plates (Figs. 5A-B, 6A-B, 7A-B). Midsternal and tergosternal junctions well-developed. Tergal anterior plates slightly bulging middorsally, while posterior ones are more flattened, giving the animal a tapering outline in lateral view, and a characteristic slender shape. Sternal plates reach their maximum width at segment 6, progressively tapering towards the posterior trunk segments. Cuticular hairs long, filiform, bracteate, abundant, arranged in a kind of three wavy transverse rows (Fig. 7E) along the tergal plate and covering two-thirds of the sternal plates. Hairs of each row surpassing the insertion of the hairs of the following row, and with hairs of the posterior row surpassing the end of the pectinate fringe. Sensory spots composed of a single pore surrounded by very few, short micropapillae

(Fig. 7D). Posterior segment margin straight, showing well-developed pectinate fringes with elongated, strongly serrated fringe tip (Fig. 7D).

Segment 1 as a closed cuticular ring (Figs. 5A-B, 6A and 7A-B), without spines and tubes. An unpaired type 1 glandular cell outlet present in middorsal position (Fig. 6F); and paired sensory spots in subdorsal and laterodorsal positions (Fig. 6F). Sensory spots on this segment are bigger than those of the remaining segments and flanked by a pair of long, filiform hairs. Ventrally, with one pair of lateroventral type 1 glandular cell outlets (Fig. 5A). Cuticular hairs on this segment scarce, mostly absent at the ventral side, and located near the sensory spots.

Segment 2 as a closed cuticular ring (Figs. 6A and 7B), without spines or tubes. A single middorsal type 1 glandular cell outlets, and paired sensory spots in subdorsal and laterodorsal (Fig. 6F) and ventromedial positions, plus one pair of ventromedial type 1 glandular cell outlets (Fig. 5A). Cuticular hairs uniformly distributed along the plate until reaching the position of the ventromedial sensory pots, absent from that point to the midventral line (Fig. 6C. F-G).

Segment 3 with unpaired middorsal type 1 glandular cell outlet, paired subdorsal sensory spots (Fig. 6F) and ventromedial type 1 glandular cell outlet. Cuticular hairs dorsally arranged similarly to that of segment 2, with a hairless midlateral area along the whole longitudinal line of the plate (Fig. 6F); ventrally with long hairs until half of the width of the plates, followed by a hairless area and a patch of short hairs closer to the midventral line (similar to Figs. 6C and 7G).

Segment 4 with a middorsal acicular spine almost reaching the posterior edge of segment 6 (Figs. 6F and 7C). Paired type 1 glandular cell outlets in paradorsal and ventromedial positions (Fig. 5A-B). Pattern of cuticular hairs similar to preceding segment.

Segment 5 without spines or sensory pots (Figs. 6F and 7C). Lateroventral pair of tubes and a ventromedial pair of type 1 glandular cell outlets (Fig. 5A). Pattern of cuticular hair similar to preceding segment.

Segment 6 with a middorsal acicular spine reaching the posterior margin of segment 8 (Fig. 6D), plus a pair of lateroventral acicular spines reaching the posterior margin of segment 7 (Fig. 6C); paired paradorsal (Fig. 7C), midlateral (Fig. 7D) and

ventromedial sensory spots (Figs. 6C and 7G). Paradorsal sensory spots located posterior to the insertion of the middorsal spine (Fig. 7C). Paired type 1 glandular cell outlets in paradorsal and ventromedial positions (Fig. 5A-B). Pattern of cuticular hairs similar to preceding segment (Fig. 7G).

Segment 7 without middorsal spines (Fig. 6D). Pairs of lateroventral acicular spines (Figs. 6C and 7D) and ventromedial type 1 glandular cell outlets. Pattern of cuticular hairs similar to preceding segment.

Segment 8 with tergal and sternal plates similar to those of segment 6 but with much longer spines (Figs. 6B, D and 7D) and with sensory spots only in paradorsal position (Fig. 5B). The middorsal spine surpasses the posterior margin of the last trunk segment (Fig. 6B), and the lateroventral ones reach the posterior end of segment 9 or even extending over the anterior half of segment 10 (Figs. 6G and 7A, D). Pattern of cuticular hairs similar to that of preceding segment but with the midventral patch of shorter hairs less developed.

Segment 9 without middorsal spine (Fig. 6D) and with a pair of long lateroventral acicular spines that reach the last trunk segment (Figs. 6G and 7A, D-F). Paired paradorsal type 1 glandular cell outlets near the anterior margin (Fig. 5B). Pairs of paradorsal, laterodorsal (Fig. 6E) and ventrolateral sensory spots (Figs. 6G and 7F), plus paired ventromedial type 1 glandular cell outlets near the anterior margin of the segment. Nephridiopore as a small sieve plate present in sublateral position (Fig. 7E).

Segment 10 with middorsal longitudinally aligned type 1 glandular cell outlets (Fig. 6E), plus one pair of paradorsal (Fig. 6E) and ventrolateral sensory spots (Figs. 6G and 7F) and ventromedial type 1 glandular cell outlets near the anterior margin of the segment. Posterior ventral segment margin curved, extending posteriorly in the ventromedial area (Figs. 6E and 7F). Cuticular hairs scarce.

Segment 11 with long lateral terminal spines, and conspicuously rounded and spatulate tergal extensions (Figs. 6A and 7F). Females with one pair of lateral terminal accessory spines, about one fifth of length of lateral terminal spines (Figs. 6A-B and 7A, F). Males with three pairs of penile spines (further details could not be distinguished in the single male specimen).

Associated kinorhynch fauna. Cephalorhyncha polunga sp. nov., and *Echinoderes* sp. 4.

3.2.5. Remarks

The new species has a spine pattern that is very common within the genus. The presence of middorsal spines on segments 4, 6 and 8 plus lateroventral spines on segments 6 to 9 is shared with 22 *Echinoderes* species. However, out of these, *Echinoderes shenlong* sp. nov. is the only species without tubes in any position on segment 2. The species is furthermore very easily recognized by its highly characteristic, broadly rounded and spatulate tergal extensions. Such tergal extensions are not described from any other species of Echinoderidae.

Regarding the *Echinoderes* diversity from bathyal depths, only 13 species are known to date: *Echinoderes bathyalis* Yamasaki, Neuhaus and George, 2018 and *Echinoderes unispinosus* Yamasaki, Neuhaus and George, 2018 were described from localities near the Azores in the Northeast Atlantic (Yamasaki et al., 2018a, b); *Echinoderes drogoni* Grzelak and Sørensen, 2017 in Grzelak and Sørensen (2018) was discovered between Svalbard and the North Pole (Grzelak and Sørensen, 2018, 2019); *Echinoderes pterus* Yamasaki, Grzelak, Sørensen, Neuhaus and George, 2018, extending from the North Pole to the Mediterranean Sea throughout the North Atlantic (Yamasaki et al., 2018c); whilst Sørensen et al. (2018) reported seven new species, and two already known species of *Echinoderes*: *Echinoderes hakaiensis* Herranz, Yangel and Leander, 2018, and *E.* cf. *unispinosus* from the Northeast Pacific. However, only *E. anniae* and *E. hamiltonorum*, both from the Northeast Pacific, fit the spine pattern of *E. shenlong* sp. nov. with middorsal spines on segments 4, 6 and 8 plus lateroventral spines on segments 6 to 9; but both show type 2 glandular cell outlets and, additionally, *E. anniae* does not have lateroventral tubes on segment 5 (Sørensen et al., 2018).

3.3. Genus *Meristoderes* Herranz et al., 2012

***Meristoderes taro* sp. nov.**

(Figs. 8-10)

ZooBank lsid: urn: lsid:zoobank.org:act:B3084423-7623-4D36-A1C7-F2479BCC4FAF.

3.3.1. Examined material

Holotype, adult male, collected in 2015, JPIO/CCZ cruise, at station MUC #86, North Pacific: 11°45.02' N, 119°39.81' W, at 4439 m depth in soft sediment; mounted in Fluoromount G®, deposited at MfN under accession number: ZMB XXXXX. 8 paratypes, 6 adult females and 2 adult males (see Table 1 for further information on stations), mounted in Fluoromount G® and deposited at the MfN under accession numbers: ZMB XXXXX–XXXXX. One additional female specimen mounted for SEM plus 4 females and 1 male mounted for LM, deposited at the MfN as additional material.

3.3.2. Diagnosis

Meristoderes with middorsal spines on segments 4-8, remarkably increasing in length on posterior segments; short laterodorsal tubes on segment 10, ventrolateral tubes on segment 2 and lateroventral tubes on segment 5, lateroventral spines on segments 6-9.

3.3.3. Etymology. The species name refers to Taro, the main character of the anime "Taro the dragon boy", by Miyoko Matsutani, one of the favourite movies during childhood of the first author. Taro searches for his mother, Tatsu, who was transformed into a dragon.

3.3.4. Description

All dimensions and measurements are summarized in Table 6, and distribution of cuticular structures in Table 7.

Head and neck. None of the specimens were suitable for introvert examinations, hence arrangement and detailed morphology of the head could not be studied. Neck with 16 trapezoidal placids of similar sizes (ca. 6 μm wide at base), except for the broader midventral one (ca. 10 μm wide at base) (Fig. 9C, D). All placids with wider bases (Figs. 9A-D and 10A-B), and separated among them by cuticular folds at the distal end. Six trichoscalid plates attached to the placids (Fig. 9D).

Trunk. 11 segments, with segment 1 as a closed cuticular ring, segment 2 partly differentiated into a tergal and a sternal plate by incomplete, intracuticular fissures between lateroventral and ventrolateral positions (Fig. 9C). Segments 2-10 with one tergal and two sternal cuticular plates, segment 11 with two sternal plates and with a middorsal fissure dividing in two the tergal plate (Figs. 8A-B, 9A-B, and 10A-B). Midsternal and tergosternal junctions well-developed. Tergal anterior plates slightly bulging middorsally, posterior ones more flattened, giving a tapering outline in lateral view. Sternal plates reach their maximum width at segment 8, progressively tapering towards the posterior trunk segments. Cuticular hairs long, filiform, bracteate (Fig. 10F) and arranged following three wavy transverse rows on most of the tergal plates, each row of hairs surpassing the perforation sites of the following row of hairs (Fig. 10 D, G-H). Ventrally, rows of cuticular hairs covering about two-thirds of the sternal plates. Sensory spots composed of a single pore surrounded by a group of short micropapillae (Fig. 10F). Posterior segment margins straight, showing primary pectinate fringes with well-developed indentations, with a more regular profile on segment 1 (Fig. 10F). Secondary pectinate fringes absent (Fig. 10F).

Segment 1 as a closed cuticular ring (Figs. 8A-B and 9C), without spines or tubes. An unpaired middorsal type 1 glandular cell outlet (Figs. 9D and 10E); and paired subdorsal and laterodorsal sensory spots (Fig. 9D). Sensory spots on this segment flanked by two to four long hairs (Fig. 10E). Ventrally, with one pair of lateroventral type 1 glandular cell outlets (Fig. 10C). Cuticular hairs on this segment are scarce, located around the sensory spots and almost absent at the ventral side (Figs. 9C, D and 10E).

Segment 2 as a cuticular ring with partially developed, intracuticular tergosternal junctions (Fig. 9C), adjacent to one pair of short ventrolateral tubes (Fig. 8A). A single middorsal type 1 glandular cell outlet and sensory spot (Fig. 10E-F), and paired sensory spots in laterodorsal (Figs. 9D and 10E) and ventromedial positions (Fig. 9C), plus one pair of ventromedial type 1 glandular cell outlets. Cuticular hairs arranged into two lines, with short hairs at the anterior band and longer ones at the posterior band (Fig. 10E-F). Hairless midlateral area along the whole longitudinal line of the plate, more evident at the following segments (see Fig. 10H). Remaining hairs uniformly distributed along the segment until reaching the ventromedial sensory pots, absent from that point to the midventral line.

Segment 3 with tergal and sternal plates with type 1 glandular cell outlet in middorsal and ventromedial positions only. Ventrally with long hairs until half of the width of the plates (Fig. 9C).

Segment 4 with a middorsal acicular spine reaching the posterior margin of the following segment (Figs. 9D and 10A). Paired type 1 glandular cell outlets in paradorsal (Fig. 9D) and ventromedial positions near the anterior margins. Pattern of cuticular hairs similar to preceding segment (Fig. 10H).

Segment 5 with tergal and sternal plates similar to those of segment 4 but with longer middorsal spine (Figs. 9A, D and 10A) and a lateroventral pair of tubes (Fig. 8A). Pattern of cuticular hairs similar to preceding segment (Fig. 10H).

Segment 6 with a middorsal spine conspicuously longer than on previous segments (Figs. 9A, D and 10A, C), reaching the posterior margin of segment 8, and with a pair of lateroventral acicular spines (Fig. 9F); plus paired paradorsal (Figs. 9D, E and 10C) and midlateral sensory spots (Figs. 9D, E and 10H-I). Paradorsal sensory spots located posterior to the insertion of the middorsal spine (Figs. 9D, E and 10C). Paradorsal and ventromedial pairs of type 1 glandular cell outlets. Pattern of cuticular hairs similar to preceding segment (Fig. 10H).

Segment 7 with middorsal (Figs. 9A, D and 10A, C, G) and lateroventral spines, both being conspicuously longer than those on previous segments (Fig. 9B, F). Type 1 glandular cell outlets in paradorsal and ventromedial positions, and sensory spots in ventromedial positions (Fig. 9F). Pattern of cuticular hairs similar to preceding segment (Fig. 10H).

Segment 8 with tergal and sternal plates similar to those of segment 6 (Fig. 9E) but with much longer spines (Figs. 9A-B, G and 10A-B, D, G), but without midlateral sensory spots. The middorsal spine extends beyond the posterior margin of the last trunk segment, and the lateroventral ones extend over the anterior half of segment 10. Pattern of cuticular hairs similar to preceding segment.

Segment 9 without middorsal spine and with a pair of long lateroventral acicular spines extending beyond the posterior margin of the last trunk segment (Figs. 9A-B, G and 10A-B, G). Paired paradorsal type 1 glandular cell outlets present. Pairs of paradorsal (Figs. 9E and 10D, G), laterodorsal (Figs. 9E and 10G) and ventrolateral

sensory spots (Fig. 9G), plus paired ventromedial type 1 glandular cell outlets aligned with those of preceding segment. Nephridiopore as a small sieve plate present in sublateral position, posterior to the insertion of the lateroventral spine (Fig. 9G). Cuticular hairs less abundant that on preceding segments, with a hairless area extending middorsally over to the subdorsal band (Fig. 10D). Otherwise similar to preceding segment.

Segment 10 with two longitudinally aligned, middorsal type 1 glandular cell outlets, short laterodorsal tubes in both sexes (Fig. 10G), plus one pair of subdorsal (Fig. 9E) and ventrolateral sensory spots (Fig. 9G) and ventromedial type 1 glandular cell outlets (Fig. 9G). Sternal plates with concave margins, extending posteriorly near the midventral junction. Otherwise similar to preceding segment.

Segment 11 with long lateral terminal spines and triangular rounded tergal extensions (Figs. 9A-B and 10A-B). Dorsal side divided in two tergal plates and with a middorsal protuberance protruding from the intersegmental joint between segments 10 and 11 (Figs. 8B, D, 9E and 10A, G). Females with one pair of lateral terminal accessory spines, about one third of length of lateral terminal spines (Fig. 10A-B). Cuticular hairs scarce at both dorsal and ventral sides. Males with three pairs of penile spines (Fig. 9A-B); ventral and dorsal penile spines filiform, midlateral penile spine coarser and slightly shorter.

Associated kinorhynch fauna. *Cephalorhyncha polunga* sp. nov., *Dracoderes toyoshioae* Yamasaki, 2015; *Echinoderes* sp. 2, *Echinoderes* sp. 4 and *Semnoderes* sp. 1.

3.3.5. Remarks

Meristoderes taro sp. nov. can be distinguished from its congeners by its spine pattern with middorsal spines on segments 4 to 8, and the remarkable increase of middorsal spine lengths from anterior towards more posterior ones. Six out of the eight currently known species of the genus have middorsal spines on segments 4, 6 and 8 only: *Meristoderes boylei* Herranz and Pardos, 2013, *Meristoderes elleae* Sørensen, Rho, Min, Kim, Chang, 2013, *Meristoderes glaber* Sørensen, Rho, Min, Kim, Chang, 2013, *Meristoderes herranzae* Sørensen, Rho, Min, Kim, Chang, 2013, *Meristoderes imugi* Sørensen, Rho, Min, Kim, Chang, 2013, and *Meristoderes macracanthus* Herranz,

Thormar, Benito, Sánchez, Pardos, 2012 (see Herranz et al., 2012; Herranz and Pardos, 2013; Sørensen et al., 2013). In addition, all these species, except for *M. glaber*, have additional tubes in the lateral series besides the lateroventral spines: *M. imugi* in sublateral position and in lateral accessory position for the remaining species (Herranz et al., 2012; Herranz and Pardos, 2013; Sørensen et al., 2013). Moreover, *M. glaber* and *M. imugi* are distinguished from *M. taro* sp. nov. by the presence of subdorsal tubes on segment 2 (Sørensen et al., 2013).

The remaining two *Meristoderes* species have middorsal spines on fewer segments, i.e., only two middorsal spines in *Meristoderes okhotensis* Adrianov and Maiorova, 2018 (segments 6 and 8) and only on segment 4 in *Meristoderes galatheae* Herranz, Thormar, Benito, Sánchez, Pardos, 2012 (Adrianov and Maiorova, 2018; Herranz et al., 2012). Additional conspicuous features to discriminate *M. taro* sp. nov. from these species are the presence of lateral accessory tubes on segment 8 in *M. galatheae* as well as pointed and prominent tergal extensions in *M. okhotensis.*

3.4. Additional kinorhynch species at the area

A total of 15 additional species were identified from 272 cores: *Campyloderes vanhöffeni*, *Condyloderes kurilensis* Adrianov and Maiorova, 2016; *Dracoderes toyoshioae*, *Echinoderes juliae*, *Fissuroderes higginsi*, *Semnoderes pacificus*, *Semnoderes* sp. 1, *Echinoderes* sp. 1, *Echinoderes* sp. 2, *Echinoderes* sp. 3, *Echinoderes* sp. 4, *Echinoderes* sp. 5, *Echinoderes* sp. 6, *Cristaphyes* sp. 1 and *Mixtophyes* sp. 1.

4. Discussion

This study showed that the soft deep sea sediment of the CCZ at the northeast Pacific harbours high kinorhynch diversity (18 species), but a relatively low abundance (723 specimens in 272 cores), as it usually occurs for other meiofaunal groups in abyssal plains and in nodule-bearing areas particularly (Glover and Smith, 2002; Lambshead et al., 2003). Of the 723 kinorhynch specimens collected at the area, most of them were juveniles (561 specimens) and hence impossible to identify species-level. Regarding the new species described herein, only one adult specimen was found in the sediment of washed nodules, specifically a specimen of *Cephalorhyncha polunga* sp. nov. This fact

suggests that none of the described species have habitat-sorting for nodules, no preference for nodule habitat.

Amongst 162 adult specimens, it was not surprising to find specimens of *Campyloderes vanhöffeni*, which has been recorded worldwide, from Faeroe Islands to Antarctica (Neuhaus and Sørensen, 2013; Zelinka, 1913); as well as *Condyloderes kurilensis*, *Dracoderes toyoshioae*, *Echinoderes juliae*, *Fissuroderes higginsi* and *Semnoderes pacificus*. All of them were described from the Pacific: *C. kurilensis* and *D. toyoshioae* from the northwest (Adrianov and Maiorova, 2016; Yamasaki, 2015), *S. pacificus* and *F. higginsi* from the southwest (Higgins, 1967; Neuhaus and Blasche, 2006). Moreover *F. higginsi* and *C. kurilensis* were recently recovered also in deep sea waters off the United States west coast (between southern Oregon and southern California) together with *Echinoderes juliae* (Sørensen et al., 2018, this issue). However, we cannot conclude whether these species have extremely wide distributions or if they actually represent cryptic species since commonly in deep-sea environments speciation does not necessary reflect changes in morphology (Janssen et al., 2015). Further molecular analysis studies seeking for gene flow and connectivity between populations must be performed in order to assess the real nature and distribution of these species and also to know whether mining activities may affect the kinorhynch biodiversity.

Such results should be cross-checked and combined with those from additional meiofaunal taxa (also macro and megafauna) and ecological data in order to understand underlying processes that allow to proper selection of areas for mining activities as well as preservation reference zones.

5. Acknowledgements

We are in debt to the Bundesanstalt für Geowissenschaften und Rohstoffe (BGR) in Hannover, to Carsten Rühlemann and Annemiek Vink who made the material from cruises MANGAN 2010 (R/V Sonne), MANGAN 2014 (R/V Kilo Moana), MANGAN 2016 (R/V Kilo Moana), FLUM (R/V Sonne) available for this study. We also wish to thank all participants and the staff involved in these seven cruises and to the staff and students of the Senckenberg Research Institute, Deutsches Zentrum für Marine Biodiversitätsforschung, Senckenberg am Meer, for sorting the specimens used herein. The EcoResponse cruise (SO239) and SO242 with R/V Sonne were financed by the

German Ministry of Education and Science (BMBF) as a contribution to the European project JPI-Oceans ‘‘Ecological Aspects of Deep-Sea Mining’’. The authors acknowledge funding from BMBF under Contract 03F0707E. The TN-319 (R/V Thomas G. Thompson) cruise was funded by UK Seabed Resources Ltd. and Ocean Minerals Singapore. We thank UK Seabed Resources Ltd for providing the necessary funds for the study of the meiofauna from this cruise.

The authors declare no conflicts of interest.

References

Adrianov, A.V., 1989. The first report on Kinorhyncha of the Sea of Japan. Zool. Zh. 61, 17–27.

Adrianov, A.V., Malakhov, V.V., 1999. Cephalorhyncha of the World Ocean. Moscow: KMK Scientific Press.

Adrianov, A.V., Maiorova, A.S., 2016. *Condyloderes kurilensis* sp. nov. (Kinorhyncha: Cyclorhagida)— a New Deep Water Species from the Abyssal Plain Near the Kuril-Kamchatka Trench. Russ. J. Mar. Biol. 42, 11–19. https://doi.org/10.1134/S1063074016010028

Adrianov, A.V., Maiorova, A.S., 2018. *Meristoderes okhotensis* sp. n. – the first deepwater representative of kinorhynchs in the Sea of Okhotsk (Kinorhyncha: Cyclorhagida). Deep Sea Res. Part. 2 Top. Stud. Oceanogr. 154, 99–105. https://doi.org/10.1016/j.dsr2.2017.10.011

Amon, D.J., Ziegler, A.F., Dahlgren, T.G., Glover, A.G., Goineau, A., Gooday, A.J., et al., 2016. Insights into the abundance and diversity of abyssal megafauna in a polymetallic-nodule region in the eastern Clarion-Clipperton Zone. Sci. Rep. 6, 30492. https://doi.org/10.1038/srep30492

De Smet, B., Pape, E., Riehl, T., Bonifácio, P., Colson, L., Vanreusel, A., 2017. The Community Structure of Deep-Sea Macrofauna Associated with Polymetallic Nodules in the Eastern Part of the Clarion-Clipperton Fracture Zone. Front. Mar. Sci. 4, 103. https://doi.org/10.3389/fmars.2017.00103

Cepeda, D., Álvarez-Castillo, L., Hermoso-Salazar, M., Sánchez, N., Gómez, S., Pardos, F., this issue. Four new species of Kinorhyncha from the Gulf of California, eastern Pacific Ocean. Zool. Anz. this issue.

Clark, A. L., Coock Clark, J., Pintz, S., 2013. Towards the Development of a Regulatory Framework for Polymetallic Nodule Exploitation in the Area. Kingston: International Seabed Authority.

Claparède, A.R.E., 1863. Zur Kenntnis der Gattung Echinoderes Duj. Beobachtungen über Anatomie und Entwicklungsgeschichte wirbelloser Thiere an der Kuste von Normandie angestellt. pp. 90–92, 119, pls. XVI–XVII. Verlag von Wilhelm Engelmann, Leipzig.

Glover, A.G., Smith, C.R., Paterson, G.L.J., Wilson, G.D.F., Hawkins, L., Sheader, M., 2002. Polychaete species diversity in the central Pacific abyss: local and regional patterns, and relationships with productivity. Mar. Ecol. Prog. Ser. 240, 157–170. https://doi.org/10.3354/meps240157

Glover, A.G., Smith, C.R., 2003. The deep-sea floor ecosystem: current status and prospects of anthropogenic change by the year 2025. Environ. Conserv. 30, 219–241. https://doi.org/10.1017/S0376892903000225

Grzelak, K., Sørensen, M.V., 2018. New species of *Echinoderes* (Kinorhyncha: Cyclorhagida) from Spitsbergen, with additional information about known Arctic species. Mar. Biol. Res. 14, 113–147. https://doi.org/10.1080/17451000.2017.1367096

Grzelak, K., Sørensen, M.V., 2019. Diversity and distribution of Arctic *Echinoderes* species (Kinorhyncha: Cyclorhagida), with the description of one new species and a redescription of *E. arlis*. Mar. Biodivers. (in press). https://doi.org/10.1007/s12526-018-0889-2

Halbach, P., Özkara, M., Hense, J., 1975. The influence of metal content on the physical and mineralogical properties of pelagic manganese nodules. Miner. Deposita. 10, 397–411. https://doi.org/10.1007/BF00207897

Halbach, P., Fellerer, R., 1980. The metallic minerals of the Pacific Seafloor. Geojournal. 4, 407–421. https://doi.org/10.1007/BF01795925

Herranz, M., Pardos, F., 2013. *Fissuroderes sorenseni* sp. nov. and *Meristoderes boylei* sp. nov.: First Atlantic recording of two rare kinorhynch genera, with new identification keys. Zool. Anz. 253, 93–111. https://doi.org/10.1016/j.jcz.2013.09.005

Herranz, M., Thormar, J., Benito, J., Sánchez, N., Pardos, F., 2012. *Meristoderes* gen.nov., a new kinorhynch genus, with the description of two new species and their

implications for echinoderid phylogeny (Kinorhyncha: Cyclorhagida, Echinoderidae). Zool. Anz. 251, 161–179. https://doi.org/10.1016/j.jcz.2011.08.004

Herranz, M., Yangel, E., Leander, B., 2018. *Echinoderes hakaiensis* sp. nov.: a new mud dragon (Kinorhyncha, Echinoderidae) from the northeastern Pacific Ocean with the redescription of *Echinoderes pennaki* Higgins, 1960. Mar. Biodivers. 48, 303–325. https://doi.org/10.1007/s12526-017-0726-z

Higgins, R.P., 1967. The Kinorhyncha of New-Caledonia. pp. 75–90 in Expedition Francaise sur les Recifs coralliens de la Nouvelle- Caledonie 2. Fondation Singer-Polignac, Paris.

Higgins, R.P., 1986. A new species of *Echinoderes* (Kinorhyncha: Cyclorhagida) from a coarse-sand California Beach. Trans. Am. Microsc. Soc. 105, 266–273. https://doi.org/10.2307/3226298

ISA-LTC, 2013. ISBA/19/LTC/8. Kingston: International Seabed Authority – Legal and Technical Commission.

Janssen, A., Kaiser, S., Meißner, K., Brenke, N., Menot, L., Arbizu, P.M., 2015. A reverse taxonomic approach to assess macrofaunal distribution patterns in abyssal Pacific polymetallic nodule fields. PLoS One. 10(2):e0117790. https://doi.org/10.1371/journal.pone.0117790

Kaiser, S., Smith, C.R., Arbizu, P.M., 2017. Editorial: Biodiversity of the Clarion Clipperton Fracture Zone. Mar. Biodivers. 47, 259–264. https://doi.org/10.1007/s12526-017-0733-0

Lambshead, P.J., Brown, C.J., Ferrero, T.J., Hawkins, L.E., Smith, C.R., Mitchell, N.J., 2003. Biodiversity of nematode assemblages from the region of the Clarion-Clipperton Fracture Zone, an area of commercial mining interest. BMC Ecol. 9, 3:1

Markhaseva, E.L., Mohrbeck, I., Renz, J., 2017. Description of *Pseudeuchaeta vulgaris* n. sp. (Copepoda: Calanoida), a new aetideid species from the deep Pacific Ocean with notes on the biogeography of benthopelagic aetideid calanoids. Mar. Biodivers. 2, 289–297. https://doi.org/10.1007/s12526-016-0527-9

Miljutin, D.M., Miljutina, M.A., Arbizu, P.M., Galéron, J., 2011. Deep-sea nematode assemblage has not recovered 26 years after experimental mining of polymetallic nodules (Clarion-Clipperton Fracture Zone, tropical eastern Pacific). Deep Sea Res. Pt I Oceanogr. Res. Pap. 58(8), 885–897. https://doi.org/10.1016/j.dsr.2011.06.003

Neuhaus, B., Blasche, T., 2006. *Fissuroderes*, a new genus of Kinorhyncha (Cyclorhagida) from the deep sea and continental shelf of New Zealand and from the

continental shelf of Costa Rica. Zool. Anz. 245, 19–52. https://doi.org/10.1016/j.jcz.2006.03.003

Neuhaus, B., Sørensen, M.V., 2013. Populations of *Campyloderes* sp. (Kinorhyncha, Cyclorhagida): one species with significant morphological variation? Zool. Anz. 252, 48–75. https://doi.org/10.1016/j.jcz.2012.03.002

Paterson, G.L., Wilson, G.D., Cosson, N., Lamont, P.A., 1998. Hessler and Jumars (1974) revisited: abyssal polychaete assemblages from the Atlantic and Pacific. Deep Sea Res. Pt. 2 Top. Stud. Oceanogr. 45, 225–251. https://doi.org/10.1016/S0967-0645(97)00084-2

Ramirez-Llodra, E., Brandt, A., Danovaro, R., De Mol, B., Escobar, E., German, C. et al., 2010. Deep, diverse and definitely different: unique attributes of the world's largest ecosystem. Biogeosciences. 7, 2851–2899. https://doi.org/10.5194/bg-7-2851-2010

Singh, R., Miljutin, D.M., Vanreusel, A., Radziejewska, T., Miljutina, M.M., Tchesunov, A., Bussau, C., Galtsova, V., Arbizu, P.M., 2016. Nematode communities inhabiting the soft deep-sea sediment in polymetallic nodule fields: do they differ from those in the nodule-free abyssal areas? Mar. Biol. Res. 12, 345–359. https://doi.org/10.1080/17451000.2016.1148822

Smith, C.R., Levin, L.A., Koslow, A., Tyler, P.A., Glover, G.G., 2008. The near future of deep seafloor ecosystems. In: Polunin, N.V.C. (ed.), Aquatic ecosystems: trends and global prospects. Cambridge University Press, Cambridge, pp. 334–351. https://doi.org/10.1017/CBO9780511751790.030

Sørensen, M.V., 2008. A new kinorhynch genus from the Antarctic deep sea and a new species of *Cephalorhyncha* from Hawaii (Kinorhyncha: Cyclorhagida: Echinoderidae). Org. Divers. Evol. 8, 230e1–230e18. https://doi.org/10.1016/j.ode.2007.11.003

Sørensen, M.V., Dal Zotto, M., Rho, H.S., Herranz, M., Sánchez, N., Pardos, F., Yamasaki, H., 2015. Phylogeny of Kinorhyncha based on morphology and two molecular loci. PLoS ONE 10(7), e0133440. https://doi.org/10.1371/journal.pone.0133440

Sørensen, M.V., Rho, H.S., Min, W.G., Kim, D., Chang, C.Y., 2013. Occurrence of the newly described kinorhynch genus *Meristoderes* (Cyclorhagida: Echinoderidae) in Korea, with the description of four new species. Helgol. Mar. Res. 67, 291–319. https://doi.org/10.1007/s10152-012-0323-2

Sørensen, M.V., Rohal, M., Thistle, D., 2018. Deep-sea Echinoderidae (Kinorhyncha: Cyclorhagida) from the Northwest Pacific. Euro. J. Taxonomy. 456, 1–75. https://doi.org/10.5852/ejt.2018.456

Sørensen, M.V., Thistle, D., Landers, S.C., this issue. North American *Condyloderes* (Kinorhyncha: Cyclorhagida: Kentrorhagata): Female dimorphism suggests moulting among adult *Condyloderes*. Zool. Anz. this issue.

Thiel, H., Schriever, G., Bussau, C., Borowski, C., 1993. Manganese nodule crevice fauna. Deep Sea Res. Pt. I Oceanogr. Res. Pap. 40, 419–423. https://doi.org/10.1016/0967-0637(93)90012-R

Vanreusel, A., Hilario, A., Ribeiro, P.A., Menot, L., Arbizu, P.M., 2016. Threatened by mining, polymetallic nodules are required to preserve abyssal epifauna. Sci. Rep. 6, 26808. https://doi.org/10.1038/srep26808

Veillette, J., Sarrazin, J., Gooday, A.J., Galéron, J., Caprais, J.C., Vangriesheim, A., et al., 2007. Ferromanganese nodule fauna in the Tropical North Pacific Ocean: species richness, faunal cover and spatial distribution. Deep Sea Res. I Oceanogr. Res. Pap. 54, 1912–1935. https://doi.org/10.1016/j.dsr.2007.06.011

Yıldız, N.Ö., Sørensen, M.V., Karaytuğ, S., 2016. A new species of *Cephalorhyncha* Adrianov, 1999 (Kinorhyncha: Cyclorhagida) from the Aegean Coast of Turkey. Helgol. Mar. Res. 70:24. https://doi.org/10.1186/s10152-016-0476-5

Yamasaki, H., 2015. Two new species of *Dracoderes* (Kinorhyncha: Dracoderidae) from the Ryukyu Islands, Japan, with a molecular phylogeny of the genus. Zootaxa. 3980, 3, 359–378. http://dx.doi.org/10.11646/zootaxa.3980.3.2

Yamasaki, H., Neuhaus, B., George, K.H., 2018a. Echinoderidae (Cyclorhagida: Kinorhyncha) from two seamounts and the adjacent deep-sea floor in the Northeast Atlantic Ocean. Cah. Biol. Mar. 59, 79–106. https://doi.org/10.21411/CBM.A.124081A9

Yamasaki, H., Neuhaus, B., George, K.H., 2018b. New species of *Echinoderes* (Kinorhyncha: Cyclorhagida) from Mediterranean Seamounts and from the deep-sea floor in the Northeast Atlantic Ocean, including notes on two undescribed species. Zootaxa. 4378, 541–566. https://doi.org/10.11646/zootaxa.4387.3.8

Yamasaki, H., Grzelak, K., Sørensen, M.V., Neuhaus, B., George, K.H., 2018c. *Echinoderes pterus* sp. n. showing a geographically and bathymetrically wide distribution pattern on seamounts and on the deep-sea floor in the Arctic Ocean, Atlantic Ocean, and the Mediterranean Sea (Kinorhyncha, Cyclorhagida). ZooKeys. 771, 15-40. https://doi.org/10.3897/zookeys.771.25534

Zelinka, C., 1894. Über die Organisation von Echinoderes Verhandlungen der Deutschen Zoologischen Gesellschaft. 4, 46–49.

Zelinka, C., 1896. Demonstration von Tafeln der Echinoderes-Monographie. Verh Dtsch Zool Gesell. 6, 197–199.

Zelinka, C., 1913. Die Echinoderen der Deutschen Südpolar-Expedition 1901-1903. Deutsche Südpolar Expedition XIV Zoologie VI: 419–437.

ACCEPTED MANUSCRIPT

Fig. 1. (A) General map of the CCZ and Peru Basin locations. (B) CCZ, with the BGR license area in grey (sampled area during the cruises MANGAN 2010, MANGAN 2014, MANGAN 2016, FLUM, JPIO/CCZ, ABYSSLINE II); sampled areas of other contractors appear in black colour (during the JPIO/CCZ cruise the western black area was also surveyed). (C) Peru Basin area surveyed during the JPIO/DISCOL cruise is highlighted in grey colour.

Fig. 2. Line art illustrations of *Cephalorhyncha polunga* sp. nov. (A) male, ventral view; (B) male, dorsal view; (C) female, ventral view of segments 10-11; (D) female, dorsal view of segments 10-11. Abbreviations: ldss, laterodorsal sensory spot; ltas, lateral terminal accessory spine; lts, lateral terminal spine; lvgco1, lateroventral type 1 glandular cell outlet; lvs, lateroventral spine; lvt, lateroventral tube; mdgco1, middorsal type 1 glandular cell outlet; mds, middorsal spine; mlgco2, midlateral type 2 glandular cell outlet; mlss, midlateral sensory spot; mlt, midlateral tube; pdgco1, paradorsal type 1 glandular cell outlet; pdss, paradorsal sensory spot; si, sieve plate; ppf, primary pectinate fringe; ps, penile spine; sdss, subdorsal sensory spot; te, tergal extension; vlss, ventrolateral sensory spot; vlt, ventrolateral tube; vmgco1, ventromedial type 1 glandular cell outlet; vmss, ventromedial sensory spot.

Fig. 3. Differential interference contrast photographs of *Cephalorhyncha polunga* sp. nov. (B-D, J) Holotypic male. (A, G-H) Paratypic females. (E) Paratypic male. (F, I, K) Additional non-type females. (A) dorsal overview; (B) ventral overview; (C) ventral view of segments 1–3; (D) detail of divisions on segment 2, ventral view; (E) midlateral to lateroventral areas in left side of segments 7–8; (F) ventral view of segment 11 showing the tergal extensions and the deeply curved posterior margin of segment 10; (G) dorsal view of segments 1–5; (H) dorsal view of segments 5–9; (I) left dorsal view of tergal plates, segments 8–11; (J) ventral view of right side sternal plates of segments 6–9; (K) ventral and right lateral views of segments 9–10. Dashed circles indicate sensory spots. Dashed line indicates midventral division of segment 2. Digits after abbreviations indicate the corresponding segment. Abbreviations: gco1/2, type 1/2 glandular cell outlet; ltas, lateral terminal accessory spine; lvs, lateroventral spine; mdpr, middorsal protuberance; mds, middorsal spine; mlt, midlateral tube; ppf, primary pectinate fringe; si, sieve plate; te, tergal extension; vlt, ventrolateral tube.

Fig. 4. SEM micrographs of female *Cephalorhyncha polunga* sp. nov. (A) dorsal view; (B) dorsolateral view; (C) dorsal view of segments 5–8; (D) right middorsal and subdorsal view of segments 2-3; (E) detail of half left lateral area of tergal plates, segment 2, showing the subdorsal type 2 glandular cell outlet and middorsal sensory spot; (F) middorsal and right lateral view of tergal plates, segments 8–9; (G) middorsal and right lateral view of tergal plates, segments 6-7; (H) left dorsal view of segment 11; (I) detail of the midlateral type 2 glandular cell outlet of segment 8, right lateral view of tergal plate. Dashed circles indicate sensory spots. Digits after abbreviations indicate the corresponding segment. Abbreviations: sdgco2, subdorsal type 2 glandular cell outlet; hr, bracteate hair; ltas, lateral terminal accessory spine; lts, lateral terminal spine; mdpr, middorsal protuberance; mds, middorsal spine; mlgco2, midlateral type 2 glandular cell outlet; ppf, primary pectinate fringe; te, tergal extension.

Fig. 5. Line art illustrations of *Echinoderes shenlong* sp. nov. (A) female, ventral view; (B) female, dorsal view; (C) male, ventral view of segments 10-11; (D) male, dorsal view of segments 10-11. Abbreviations: ldss, laterodorsal sensory spot; ltas, lateral terminal accessory spine; lts, lateral terminal spine; lvgco1, lateroventral type 1 glandular cell outlet; lvs, lateroventral spine; lvt, lateroventral tube; mdgco1, middorsal type 1 glandular cell outlet; mds, middorsal spine; mlss, midlateral sensory spot; pdgco1, paradorsal type 1 glandular cell outlet; pdss, paradorsal sensory spot; ppf, primary pectinate fringe; ps, penile spine; sdss, subdorsal sensory spot; si, sieve plate; te, tergal extension; vlss, ventrolateral sensory spot; vmgco1, ventromedial type 1 glandular cell outlet; vmss, ventromedial sensory spot.

Fig. 6. Differential interference contrast photographs of *Echinoderes shenlong* sp. nov. (A-B, D, F) Holotypic male. (C, E, G) Paratypic female. (A) ventral overview; (B) dorsal overview; (C) ventral view of segments 6–8; (D) dorsal view of segments 6–9; (E) dorsal view of segments 9–10; (F) dorsal view of segments 1–6; (G) ventral view of segments 9–11. Dashed circles indicate sensory spots. Digits after abbreviations indicate the corresponding segment. Abbreviations: gco1, type 1 glandular cell outlet; lvs, lateroventral spine; mds, middorsal spine; pl, placid.

Fig. 7. SEM micrographs of female of *Echinoderes shenlong* sp. nov. (A) dorsolateral view; (B) ventral view; (C) left lateral view of tergal plates, showing middorsal, paradorsal and subdorsal areas of segments 4–6; (D) left lateral view of tergal plates,

segments 6–9; (E) detail of the left lateral area of tergal plate, segment 9; (F) ventral and lateroventral view of segments 9–11; (G) right sternal plate of segment 6. Dashed circles indicate sensory spots. Digits after abbreviations indicate the corresponding segment. Abbreviations: hr, bracteated hair; ltas, lateral terminal accessory spine; lts, lateral terminal spine; lvs, lateroventral spine; mds, middorsal spine; ppf, primary pectinate fringe; sh, short hairs; si, sieve plate; te, tergal extension; vlss, ventrolateral sensory spot; vmss, ventromedial sensory spot.

Fig. 8. Line art illustrations of *Meristoderes taro* sp. nov. (A) female, ventral view; (B) female, dorsal view; (C) male, ventral view of segments 10-11; (D) male, ventral view of segments 10-11. Abbreviations: ldss, laterodorsal sensory spot; ldt, laterodorsal tube; ltas, lateral terminal accessory spine; lts, lateral terminal spine; lvgco1, lateroventral type 1 glandular cell outlet; lvs, lateroventral spine; lvt, lateroventral tube; mds, middorsal spine; mlss, midlateral sensory spot; mdgco1, middorsal type 1 glandular cell outlet; pdgco1, paradorsal type 1 glandular cell outlet; pdss, paradorsal sensory spot; ppf, primary pectinate fringe; ps, penile spine; sdss, subdorsal sensory spot; si, sieve plate; te, tergal extension; vlss, ventrolateral sensory spot; vlt, ventrolateral tube; vmgco1, ventromedial type 1 glandular cell outlet; vmss, ventromedial sensory spot.

Fig. 9. Differential interference contrast photographs of *Meristoderes taro* sp. nov. (A-B, D, F) Holotypic male. (C, E, G) Paratypic females. (A) dorsal overview; (B) ventral overview; (C) ventral view of segments 1–3; (D) dorsal view of segments 1–7; (E) dorsal view of segments 6–11; (F) ventral and lateroventral views of segments 6–7; (G) ventral, lateroventral and sublateral view of segments 9–11. Dashed circles indicate sensory spots. Dashed lines indicate partial divisions of segment 2 in C and middorsal fissure on segment 11 in E. Arrow head indicates the middorsal protuberance. Digits after abbreviations indicate the corresponding segment. Abbreviations: gco1, type 1 glandular cell outlet; lvs, lateroventral spine; mds, middorsal spine; mvpl, midventral placid; pl, placid; si, sieve plate; tp, trichoscalid plate.

Fig. 10. SEM micrographs of females of *Meristoderes taro* sp. nov. (A) dorsal view; (B) right dorsolateral view; (C) middorsal and paradorsal view of segments 6–7; (D) dorsal, paradorsal, subdorsal and laterodorsal view of segments 8–9; (E) dorsal view of segments 1–4; (F) detail of middorsal and paradorsal areas of segments 2-3, showing the middorsal sensory spot of segment 2; (G) right side of tergal plates of segments 8–

11; (H) half right of tergal plates of segments 4–7; (I) detail of midlateral sensory spot of segment 6. Dashed circles indicate sensory spots. Digits after abbreviations indicate the corresponding segment. Abbreviations: gco1, type 1 glandular cell outlet; hr, bracteated hair; ldt, laterodorsal tube; lvs, lateroventral spine; mdpr, middorsal protuberance; mds, middorsal spine; mlss, midlateral sensory spot; ppf, pectinate fringe.

ACCEPTED MANUSCRIPT

ACCEPTED MANUSCRIPT

Table 1. Summary of data on stations and catalogue numbers for specimens of the new species.

Cruise	Station / Core	Collecting date	Latitude, Longitude	Depth (m)	Mounting	Type status and number of specimens
Mangan 2010	TV-MUC #13 / 04	28/4/10	11°19.16' N 119°18.433' W	4325	LM	1♂ paratype *Meristoderes taro* sp. nov.
Mangan 2010	MUC #23 / 12	1/5/10	11°35.416' N 116°11.294' W	4210	LM	1♂ paratype *Cephalorhyncha polunga* sp. nov.
Mangan 2010	MUC #23 / 12 (Nodule)	1/5/10	11°35.416' N 116°11.294' W	4210	LM	1♂ paratype *Cephalorhyncha polunga* sp. nov.
Mangan 2010	MUC #48 / 11	7/5/10	11°57.316' N 116°58.518' W	4106	LM	1♂ *Cephalorhyncha polunga* sp. nov.
Mangan 2010	MUC #48 / 12	7/5/10	11°57.316' N 116°58.518' W	4106	LM LM	1♂ *Cephalorhyncha polunga* sp. nov. 1 *Echinoderes* sp. 4
Mangan 2014	MUC #82 / 06	21/5/14	11°15.635' N 117°15.882' W	4196	LM LM	1♀ paratype *Cephalorhyncha polunga* sp. nov. 1 *Echinoderes* sp. 4
Flum 2015	MUC #37 / 05	18/5/15	12°54.131' N 118°24.782' W	4319	LM	1♀ holotype *Echinoderes shenlong* sp. nov.
Flum 2015	MUC #61 / 05	25/5/15	12°56.109' N 119°08.871' W	4293	LM LM	1♀ paratype *Echinoderes shenlong* sp. nov. 1 *Echinoderes* sp. 4
Flum 2015	MUC #68 / 12	27/5/15	119°11.514' W 12°40.307' N	4408	LM	1♂ paratype *Cephalorhyncha polunga* sp. nov.
Flum 2015	MUC #74 / 11	29/5/15	12°55.601' N 119°08.83' W	4295	LM LM LM	1♂ *Cephalorhyncha polunga* sp. nov. 1 *Echinoderes* sp. 1 1 *Echinoderes* sp. 2
Flum 2015	MUC #95 / 04	5/6/15	11°49.262' N 117°13.197' W	4150	LM	1♀ paratype *Cephalorhyncha polunga* sp. nov.
Flum 2015	MUC #109 / 12	8/6/15	11°48.791' N 116°31.76' W	4327	LM LM LM SEM	1♂ holotype *Cephalorhyncha polunga* sp. nov. 1♀ *Cephalorhyncha polunga* sp. nov. 1 *Semnoderes pacificus* 1 *Campyloderes vanhöffeni*
JPIO/CCZ	MUC #67 / 12	30/3/15	11°49.37' N 117°32.00' W	4347	LM	1♀ paratype *Cephalorhyncha polunga* sp. nov.
JPIO/CCZ	MUC #71 / 03	31/3/15	11°47.88' N 117°30.62' W	4354	LM	1♀ paratype *Meristoderes taro* sp. nov.
JPIO/CCZ	MUC #71 / 04	31/3/15	11°47.88' N 117°30.62' W	4354	SEM	1♀ *Meristoderes taro* sp. nov.
JPIO/CCZ	MUC #86 / 04	2/4/15	11°45.02' N 119°39.81' W	4439	LM	1♂ holotype *Meristoderes taro* sp. nov.
JPIO/CCZ	MUC #91 / 10	3/4/15	11°04.39' N 119°39.34' W	4419	LM SEM	1♀ *Cephalorhyncha polunga* sp. nov. 1 *Echinoderes* sp. 4
JPIO/CCZ	MUC #164 / 08	16/4/15	14°03.00' N 130°07.42' W	4955	LM	1♀ *Cephalorhyncha polunga* sp. nov.
JPIO/CCZ	MUC #176 / 11	18/4/15	14°02.54' N 130°05.13' W	5012	SEM LM	1♀ *Cephalorhyncha polunga* sp. nov. 1 *Echinoderes* sp. 4
JPIO/CCZ	MUC #202 / 11	23/4/15	18°47.35' N 128°21.26' W	4835	LM	1♀ *Cephalorhyncha polunga* sp. nov.
Mangan 2016	MUC #47 / 06	3/5/16	11°50.214' N 116°58.391' W	4090	LM	1♂ paratype *Cephalorhyncha polunga* sp. nov.

ACCEPTED MANUSCRIPT

ACCEPTED MANUSCRIPT

Mangan 2016	MUC #52 / 02	4/5/16	11°49.257' N 117°04.05' W	4156	LM	1♀ *Cephalorhyncha polunga* sp. nov.
Mangan 2016	MUC #90 / 04	8/5/16	11°49.589' N 117°30.952' W	4363	LM	1♀ paratype *Meristoderes taro* sp. nov.
Mangan 2016	MUC #90 / 10	8/5/16	11°49.589' N 117°30.952' W	4363	LM	1♀ paratype *Meristoderes taro* sp. nov.
Mangan 2016	MUC #100 / 05	10/5/16	11°54.735' N 117°29.122' W	4195	LM	1♀ paratype *Cephalorhyncha polunga* sp. nov.
Mangan 2016	MUC #102 / 01	11/5/16	11°49.155' N 117°33.118' W	4334	LM	1♀ paratype *Meristoderes taro* sp. nov.
Mangan 2016	MUC #102 / 04	11/5/16	11°49.155' N 117°33.118' W	4334	LM LM	1♀ paratype *Cephalorhyncha polunga* sp. nov. 1♀ *Meristoderes taro* sp. nov.
Mangan 2016	MUC #104 / 09	11/5/16	11°53.795' N 117°27.905' W	4202	LM LM	1♀ paratype *Meristoderes taro* sp. nov. 1♂ *Meristoderes taro* sp. nov.
JPIO/DISCOL	35-MUC-07 / 10	3/8/15	07°07.54' S 088°27.03' W	4160	LM LM LM	1♂ paratype *Meristoderes taro* sp. nov. 1 *Echinoderes* sp. 4 1 *Dracoderes toyoshioae*
JPIO/DISCOL	39-MUC-08 / 12	3/8/15	07°07.52' S 088°27.03' W	4163	LM	1♀ *Cephalorhyncha polunga* sp. nov.
JPIO/DISCOL	40-MUC-09 / 09	3/8/15	07°07.54' S 088°27.02' W	4164	LM LM	1♂ paratype *Echinoderes shenlong* sp. nov. 1 *Echinoderes* sp. 4
JPIO/DISCOL	46-MUC-11 / 10	5/8/15	07°07.53' S 088°27.01' W	4162	LM	1♀ paratype *Echinoderes shenlong* sp. nov.
JPIO/DISCOL	56-MUC-12 / 07	6/8/15	07°04.35' S 088°27.64' W	N/A	LM	1♀ *Cephalorhyncha polunga* sp. nov.
JPIO/DISCOL	62-MUC-14 / 08	7/8/15	07°04.42' S 088°27.86' W	4154	LM SEM LM SEM	1♀ *Meristoderes taro* sp. nov. 1 *Echinoderes* sp. 4 1 *Echinoderes* sp. 4 1 *Semnoderes* sp. 1
JPIO/DISCOL	64-MUC-15 / 11	7/8/15	07°04.42' S 088°27.85' W	4153	SEM	1♀ *Echinoderes shenlong* sp. nov.
JPIO/DISCOL	73-MUC-19 / 11	11/8/15	07°04.41' S 088°27.89' W	4121	LM LM LM	1♀ *Cephalorhyncha polunga* sp. nov. 1♀ paratype *Echinoderes shenlong* sp. nov. 1 *Echinoderes* sp. 4
JPIO/DISCOL	91-MUC-24 / 11	15/8/15	07°04.58' S 088°31.56' W	4127	LM	1♀ paratype *Meristoderes taro* sp. nov.
JPIO/DISCOL	92-MUC-25 / 09	15/8/15	07°04.56' S 088°31.57' W	4127	LM LM	1♀ *Meristoderes taro* sp. nov. 1 *Semnoderes* sp. 1
JPIO/DISCOL	109-MUC-27 / 12	18/8/15	07°04.49' S 088°26.84' W	4161	LM LM	1♀ *Meristoderes taro* sp. nov. 1 *Echinoderes* sp. 2
JPIO/DISCOL	110-MUC-28 / 09	18/8/15	07°04.45' S 088°26.77' W	4175	LM	1♀ *Cephalorhyncha polunga* sp. nov.
Abyssline II	MC02 / 02	2015	12°22.024' N 116°31.020' W	4150	LM LM	1♀ *Cephalorhyncha polunga* sp. nov. *Fissuroderes higginsi*

Table 2. Measurements (µm) and proportions of *Cephalorhyncha polunga* sp. nov. Numbers in the first column indicate the corresponding segment. Abbreviations: LTAS, lateral terminal accessory spine; LTS, lateral terminal spine; LV, lateroventral spine/tube; MD, middorsal spine; MSW, maximum sternal width, measured on segment 7; n, number of measured specimens; S, segment length; SD, standard deviation; SW, standard width, measured on segment 10; TL, total trunk length.

	Holotype	n	Mean ♂	Mean ♀	Mean	Range	SD
TL	387	5♂/5♀	382	372	377	300 - 432	43,12
MSW 7	76	5♂/5♀	74	73	73.5	64 - 77	4,13
MSW/TL	20%	5♂/5♀	19%	20%	19.5%	17% – 23%	1,73%
SW10	63	5♂/5♀	62	61	61.5	54 - 64	3,73
S1	40	5♂/5♀	40	39	40	34 - 43	2,42
S2	33	5♂/5♀	34	33	33	30 - 37	2,31
S3	32	5♂/5♀	32	32	32	28 - 36	2,00
S4	36	5♂/5♀	35	36	35	33 - 37	1,10
S5	37	5♂/5♀	37	38	37	33 - 44	3,03
S6	43	5♂/5♀	41	41	41	36 - 44	2,65
S7	48	5♂/5♀	46	45	46	41 - 48	2,38
S8	52	5♂/5♀	53	49	51	47 - 55	2,56
S9	55	5♂/5♀	56	54	55	52 - 60	2,75
S10	60	5♂/5♀	61	72	60	52 - 64	3,70
S11	59	5♂/3♀	60	46	61	59 - 63	1,55
MD4	24	4♂/5♀	29	30	29	24 - 31	2,26
MD5	33	5♂/4♀	35	36	35	32 - 40	2,73
MD6	-	5♂/5♀	30	41	36	32 - 51	5,39
MD7	48	5♂/5♀	51	56	53	48 - 67	5,77
MD8	68	5♂/5♀	78	89	83	68 - 117	15,47
LV2	27	3♂/5♀	27	20	23	18 - 31	4,24
LV5	23	5♂/5♀	25	18	21	13 - 27	4,27
LV6	34	5♂/5♀	37	39	38	33 - 50	4,89
LV7	58	5♂/5♀	53	49	51	45 - 58	4,44
LV8	60	5♂/5♀	59	57	58	54 - 62	3,16
LV9	64	5♂/5♀	68	65	66	62 - 72	3,68
LTS	233	4♂/5♀	242	238	240	226 - 257	10,23
LTAS	-	5♀	-	69	-	64 - 73	3,54
LTS/TL	60%	4♂/5♀	63%	65%	64%	53% - 83%	22,19%

ACCEPTED MANUSCRIPT

Table 3. Summary of relevant cuticular characters and positions of *Cephalorhyncha polunga* sp. nov. Abbreviations: LA, lateral accessory; LD, laterodorsal; LV, lateroventral; ML, midlateral; MD, middorsal; PD, paradorsal; SD, subdorsal; SL, sublateral; VL, ventrolateral; VM, ventromedial; ac, acicular spine; gco1/2, type 1/2 glandular cell outlet; ltas, lateral terminal accessory spine; lts, lateral terminal spine; pr, protuberance; ps, penile spine; si, sieve plate; ss, sensory spot; t, tube; ♂, male condition of sexually dimorphic characters; ♀, female condition of sexually dimorphic characters.

Position Segment	**MD**	**PD**	**SD**	**LD**	**ML**	**SL**	**LA**	**LV**	**VL**	**VM**
1	gco1		ss	ss				gco1	gco1	
2	gco1, ss		gco2	ss	ss				t	gco1, ss
3	gco1		ss							gco1
4	ac	gco1								gco1
5	ac	gco1		ss				t		gco1
6	ac	gco1, ss			ss			ac		gco1
7	ac	gco1, ss						ac		gco1, ss
8	ac	gco1, ss			gco2			ac		gco1
9		gco1, ss	ss	ss		si		ac	ss	gco1
10	gco1, gco1	ss			t				ss	gco1
11	pr		ss		3xps(♂)		ltas(♀)	lts	ss	

ACCEPTED MANUSCRIPT

Table 4. Measurements (µm) and proportions of *Echinoderes shenlong* sp. nov. Numbers in the first column indicate the corresponding segment. Abbreviations: LTAS, lateral terminal accessory spine; LTS, lateral terminal spine; LV, lateroventral spine/tube; MD, Middorsal spine; MSW, maximum sternal width, measured on segment 6; n, number of measured specimens; S, segment length; SD, standard deviation; SW, standard width, measured on segment 10; TL, total trunk length.

	Holotype	**n**	♂	**Mean ♀**	**Mean**	**Range**	**SD**
TL	218	1♂/4♀	188	218	212	188 - 232	16,8
MSW 6	54	4♀	-	54	54	53 - 54	0,68
MSW/TL	25%	3♀	-	25%	25%	23% – 26%	1,24%
SW10	44	3♀	-	42	42	41 - 44	1,86
S1	29	4♀	-	28	28	25 - 29	1,94
S2	28	4♀	-	21	21	18 - 28	4,35
S3	21	4♀	-	20	20	19 - 22	1,25
S4	22	4♀	-	22	22	21 - 24	1,47
S5	24	4♀	-	24	24	22 - 25	1,39
S6	26	4♀	-	26	26	24 - 27	1,22
S7	27	4♀	-	27	27	27 - 28	0,69
S8	32	3♀	-	32	32	31 - 32	0,71
S9	34	3♀	-	34	34	32 - 35	1,47
S10	39	3♀	-	37	37	33 - 39	3,44
S11	23	2♀	-	21	21	19 - 23	3,16
MD4	30	1♂/4♀	48	41	43	30 - 50	7,94
MD6	65	1♂/3♀	83	64	68	62 - 83	9,81
MD8	92	1♂/4♀	111	101	103	92 - 113	9,69
LV5	-	2♀	-	13	13	11 - 15	2,52
LV6	30	1♂/4♀	34	32	33	30 - 36	2,72
LV7	36	1♂/4♀	45	35	37	31 - 45	5,17
LV8	43	1♂/4♀	57	46	48	43 - 57	6,29
LV9	52	1♂/4♀	60	56	56	51 - 63	5,11
LTS	199	1♂/4♀	244	214	220	180 - 244	28,36
LTAS	50	4♀	-	46	-	44 - 50	2,72
LTS/TL	91%	1♂/4♀	130%	98%	104%	88%-130%	16,78%

ACCEPTED MANUSCRIPT

Table 5. Summary of relevant cuticular characters and positions of *Echinoderes shenlong* sp. nov. Abbreviations: LA, lateral accessory; LD, laterodorsal; LV, lateroventral; ML, midlateral; MD, middorsal; PD, paradorsal; SD, subdorsal; SL, sublateral; VL, ventrolateral; VM, ventromedial; ac, acicular spine; gco1, glandular cell outlet type 1; ltas, lateral terminal accessory spine; lts, lateral terminal spine; ps, penile spine; si, sieve plate; ss, sensory spot; t, tube; ♂, male condition of sexually dimorphic characters; ♀, female condition of sexually dimorphic characters.

Position Segment	**MD**	**PD**	**SD**	**LD**	**ML**	**SL**	**LA**	**LV**	**VL**	**VM**
1	gco1		ss	ss				gco1		
2	gco1		ss	ss						gco1, ss
3	gco1		ss							gco1
4	ac	gco1								gco1
5								t		gco1
6	ac	gco1, ss			ss			ac		gco1, ss
7								ac		gco1
8	ac	gco1, ss						ac		gco1
9		gco1, ss		ss		si		ac	ss	gco1
10	gco1, gco1	ss							ss	gco1
11					3xps(♂)		ltas(♀)	lts		

ACCEPTED MANUSCRIPT

Table 6. Measurements (µm) and proportions of *Meristoderes taro* sp. nov. Numbers in the first column indicate the corresponding segment. Abbreviations: LTAS, lateral terminal accessory spine; LTS, lateral terminal spine; LV, lateroventral spine; MD, Middorsal spine; MSW, maximum sternal width, measured on segment 8; n, number of measured specimens; S, segment length; SD, standard deviation; SW, standard width, measured on segment 10; TL, total trunk length; VL, ventrolateral tube.

	Holotype	**n**	**Mean ♂**	**Mean ♀**	**Mean**	**Range**	**SD**
TL	251	3♂/6♀	244	267	260	218 - 288	19,02
MSW 8	58	2♂/4♀	58	57	57	56 - 58	1,04
MSW/TL	23%	2♂/4♀	24%	21%	22%	21% – 23%	0,92%
SW10	50	2♂/4♀	48	47	47	29 - 50	1,96
S1	31	2♂/5♀	30	33	32	19 - 38	3,23
S2	28	2♂/5♀	23	24	24	19 - 27	3,93
S3	22	2♂/5♀	23	24	24	22 - 26	1,69
S4	27	2♂/5♀	26	28	28	27 - 30	1,40
S5	28	2♂/5♀	28	30	30	28 - 34	2,49
S6	31	2♂/5♀	31	33	33	31 - 38	2,02
S7	34	2♂/5♀	36	37	36	34 - 39	1,93
S8	35	2♂/5♀	37	39	38	33 - 42	2,25
S9	33	2♂/5♀	37	39	38	35 - 42	3,31
S10	35	2♂/5♀	35	37	36	34 - 43	2,84
S11	25	2♂/4♀	25	23	23	18 - 25	2,76
MD4	37	3♂/5♀	43	44	44	38 - 47	3,32
MD5	46	3♂/3♀	50	51	51	46 - 55	3,38
MD6	67	3♂/4♀	69	69	69	58 - 83	7,92
MD7	113	2♂/4♀	97	93	94	80- 113	12,47
MD8	151	2♂/4♀	135	127	129	107 - 151	15,15
VL2	-	3♀	-	16	16	11 - 22	5,58
LV5	10	1♂/5♀	10	12	12	10 - 16	2,90
LV6	40	1♂/5♀	40	47	46	40 - 49	3,18
LV7	62	2♂/5♀	62	57	58	56 - 62	4,00
LV8	71	3♂/5♀	69	64	66	55- 71	4,57
LV9	86	3♂/5♀	82	77	79	65 - 86	7,14
LTS	227	3♂/5♀	216	206	210	194 - 227	13,18
LTAS	-	5♀	-	74	-	71 -78	2,81
LTS/TL	90%	3♂/6♀	89%	77%	81%	71% - 91%	8,06%

ACCEPTED MANUSCRIPT

ACCEPTED MANUSCRIPT

Table 7. Summary of relevant cuticular characters and positions of *Meristoderes taro* sp. nov. Abbreviations: LA, lateral accessory; LD, laterodorsal; LV, lateroventral; ML, midlateral; MD, middorsal; PD, paradorsal; SD, subdorsal; SL, sublateral; VL, ventrolateral; VM, ventromedial; ac, acicular spine; gco1, glandular cell outlet type 1; ltas, lateral terminal accessory spine; lts, lateral terminal spine; pr, protuberance; ps, penile spine; si, sieve plate; ss, sensory spot; t, tube; ♂, male condition of sexually dimorphic characters; ♀, female condition of sexually dimorphic characters.

Position Segment	**MD**	**PD**	**SD**	**LD**	**ML**	**SL**	**LA**	**LV**	**VL**	**VM**
1	gco1		ss	ss				gco1		
2	gco1, ss			ss					t	gco1, ss
3	gco1									gco1
4	ac	gco1								gco1
5	ac	gco1						t		gco1
6	ac	gco1, ss			ss			ac		gco1
7	ac	gco1						ac		gco1, ss
8	ac	gco1, ss						ac		gco1
9		gco1, ss		ss		si		ac	ss	gco1
10	gco1, gco1		ss	t					ss	gco1
11	pr				3xps(♂)		ltas(♀)	lts		

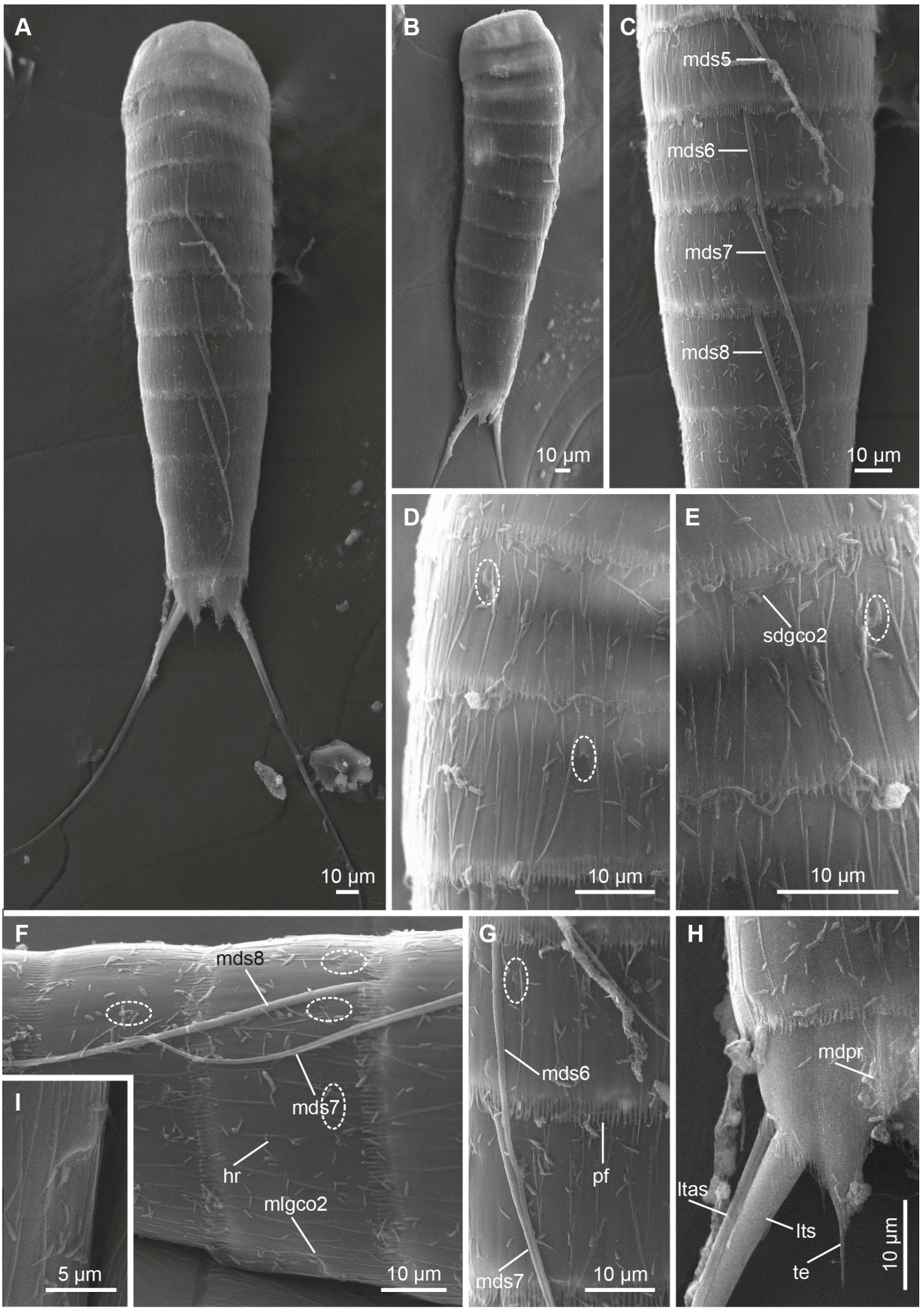
A
B
C
mds5
mds6
mds7
mds8
10 µm
10 µm
10 µm
D
E
sdgco2
10 µm
10 µm
F
mds8
mds7
hr
mlgco2
10 µm
I
5 µm
G
mds6
pf
mds7
10 µm
H
mdpr
ltas
lts
te
10 µm

ACCEPTED MANUSCRIPT

ACCEPTED MANUSCRIPT

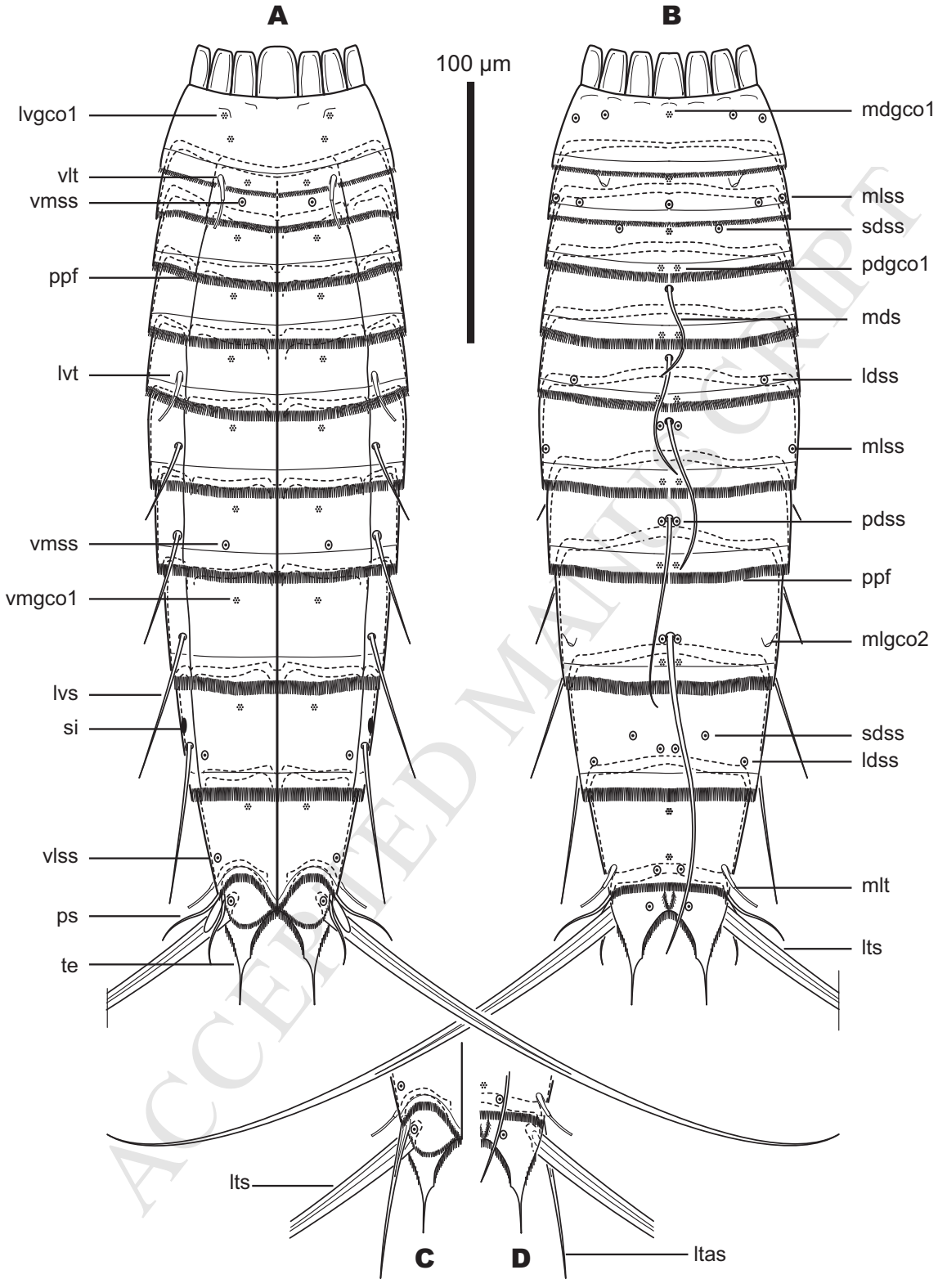

ACCEPTED MANUSCRIPT

ACCEPTED MANUSCRIPT

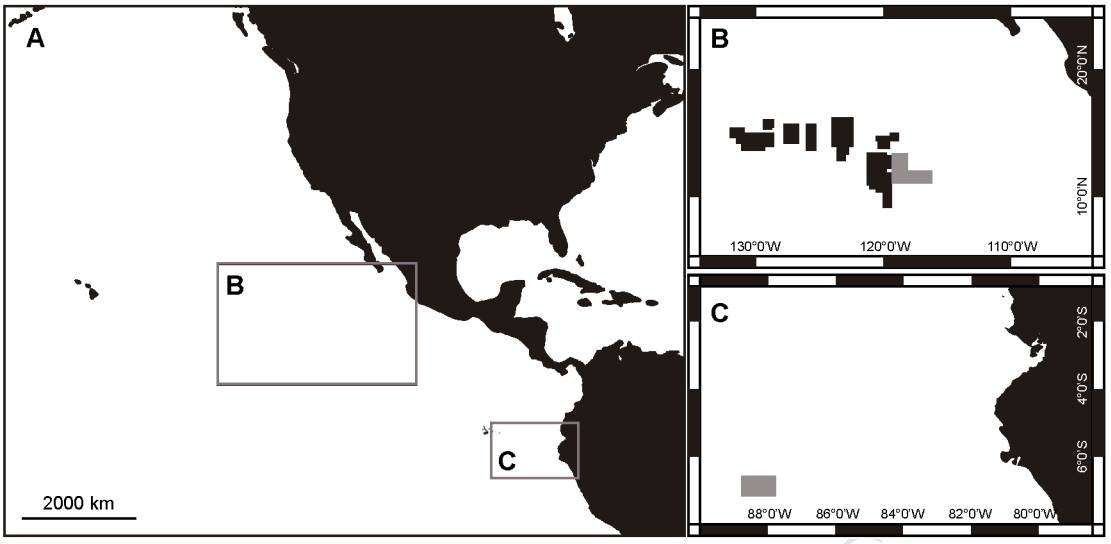

ACCEPTED MANUSCRIPT

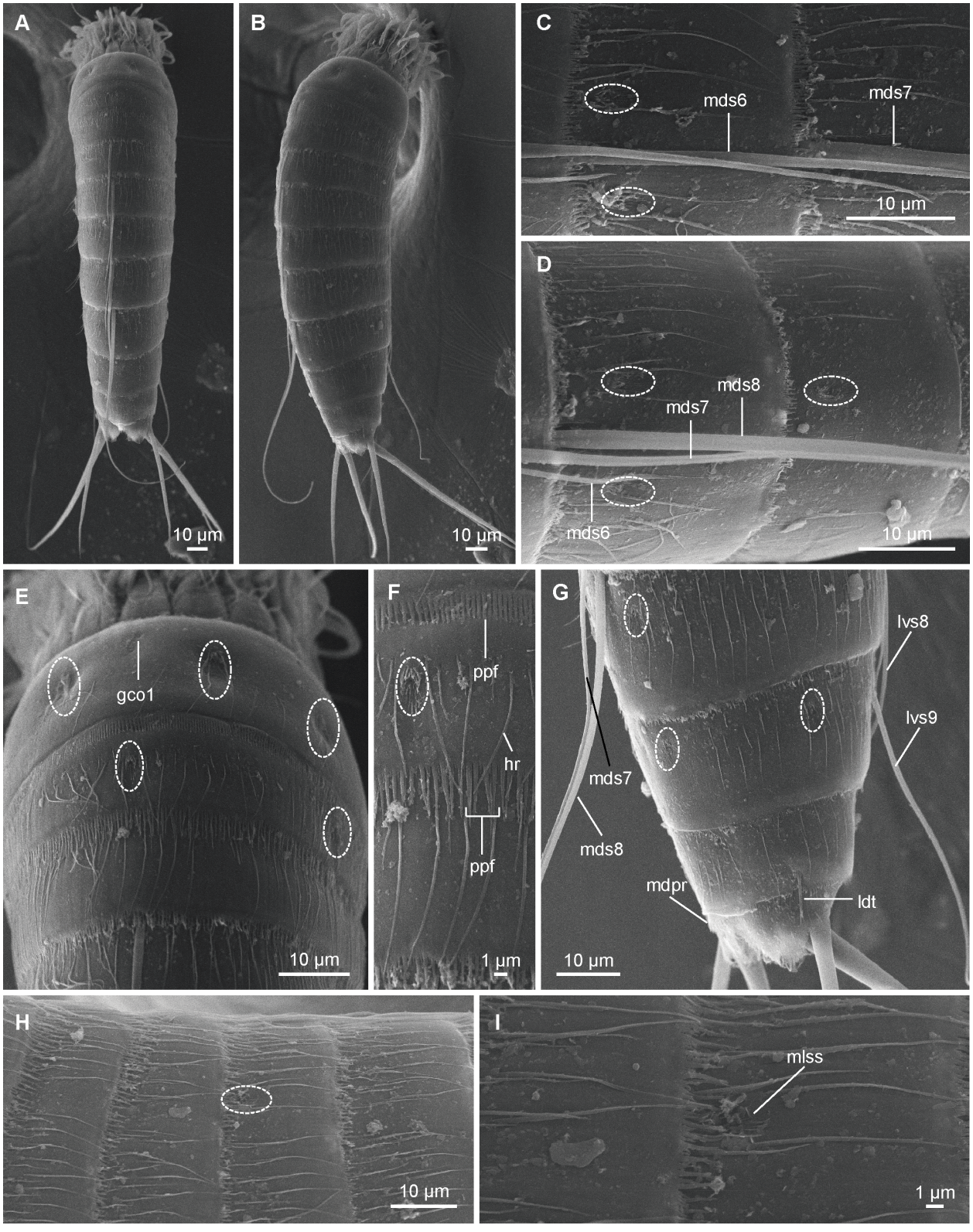
A
10 µm
B
10 µm
C
mds6
mds7
10 µm
D
mds8
mds7
mds6
10 µm
E
gco1
10 µm
F
ppf
hr
ppf
1 µm
G
lvs8
lvs9
mds7
mds8
mdpr
ldt
10 µm
H
10 µm
I
mlss
1 µm

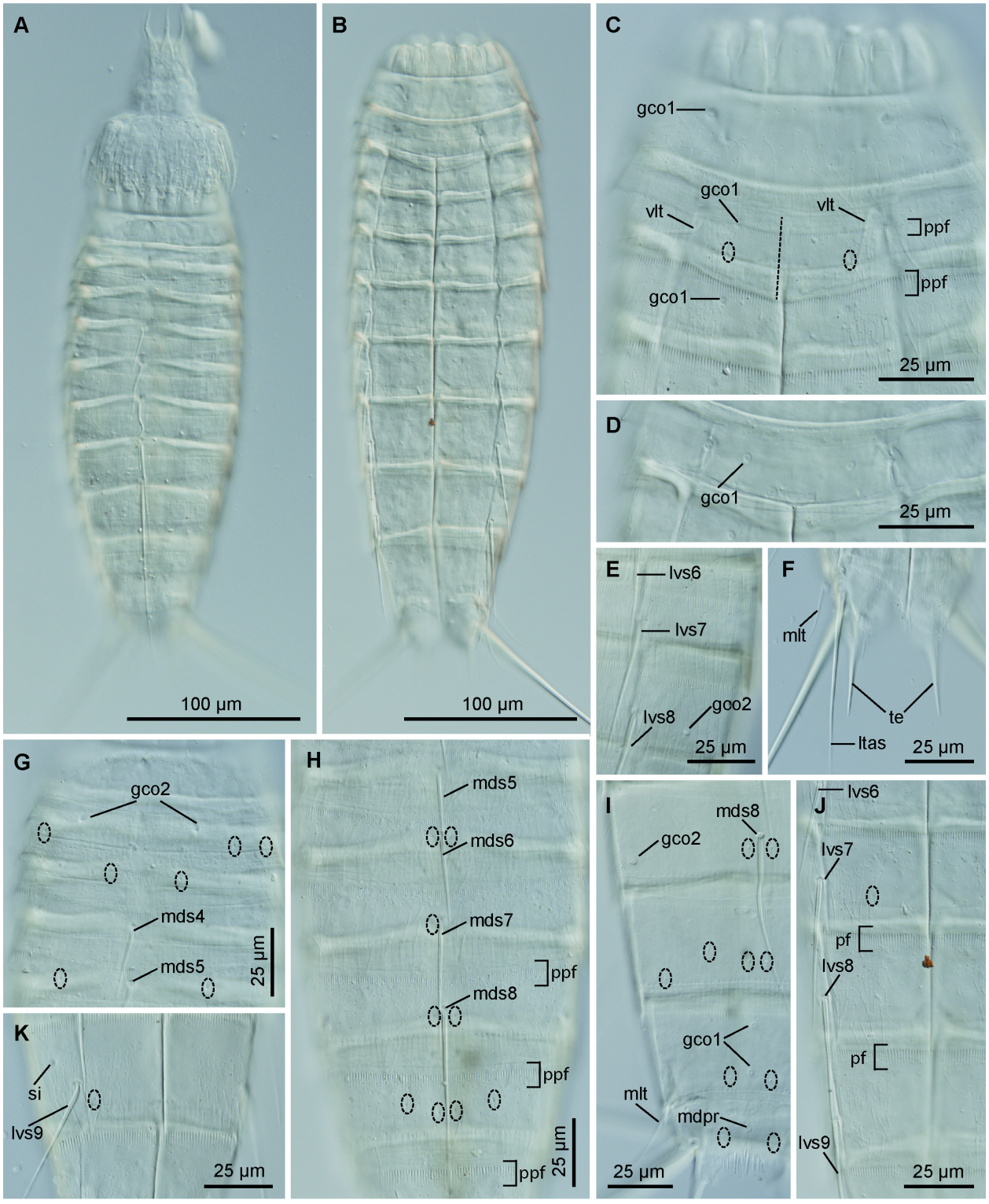
A
100 µm
B
100 µm
C
gco1
gco1
vlt
vlt
ppf
ppf
gco1
25 µm
D
gco1
25 µm
E
lvs6
lvs7
lvs8
gco2
25 µm
F
mlt
te
ltas
25 µm
G
gco2
mds4
mds5
25 µm
H
mds5
mds6
mds7
ppf
mds8
ppf
ppf
25 µm
I
mds8
gco2
gco1
mlt
mdpr
25 µm
J
lvs6
lvs7
pf
lvs8
pf
lvs9
25 µm
K
si
lvs9
25 µm

ACCEPTED MANUSCRIPT

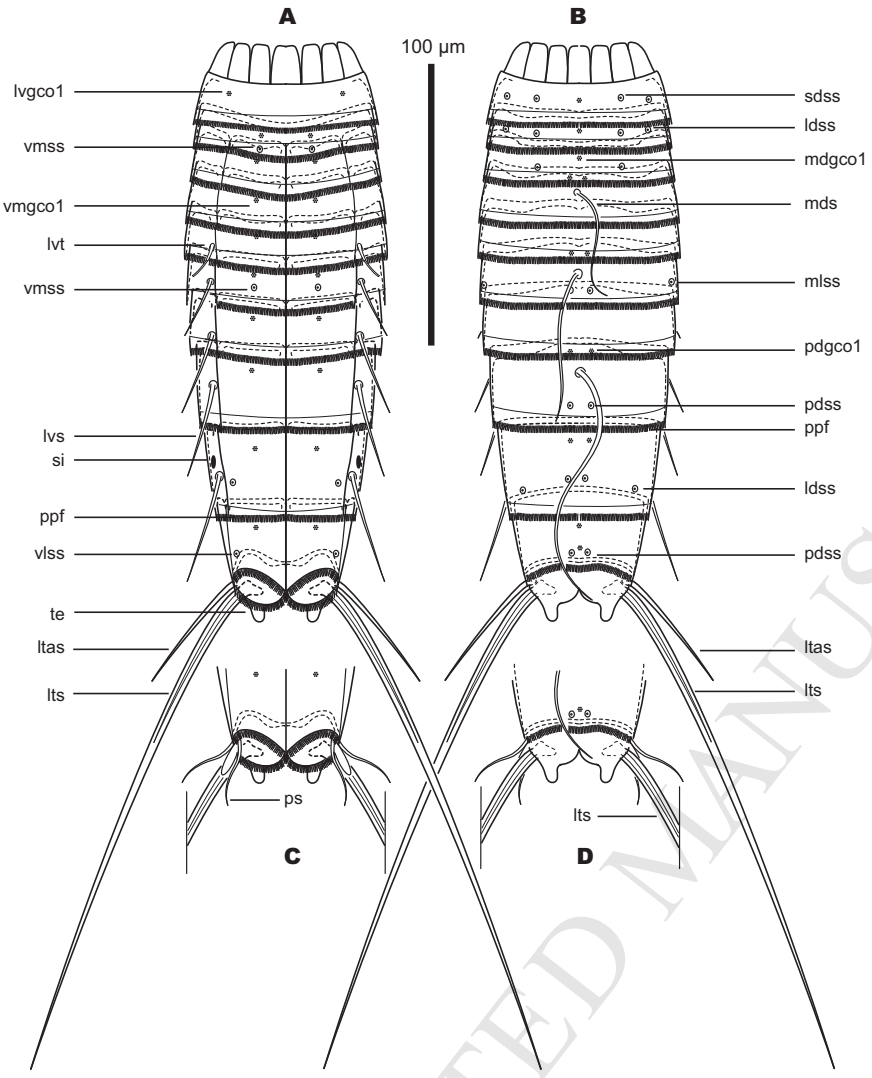

ACCEPTED MANUSCRIPT

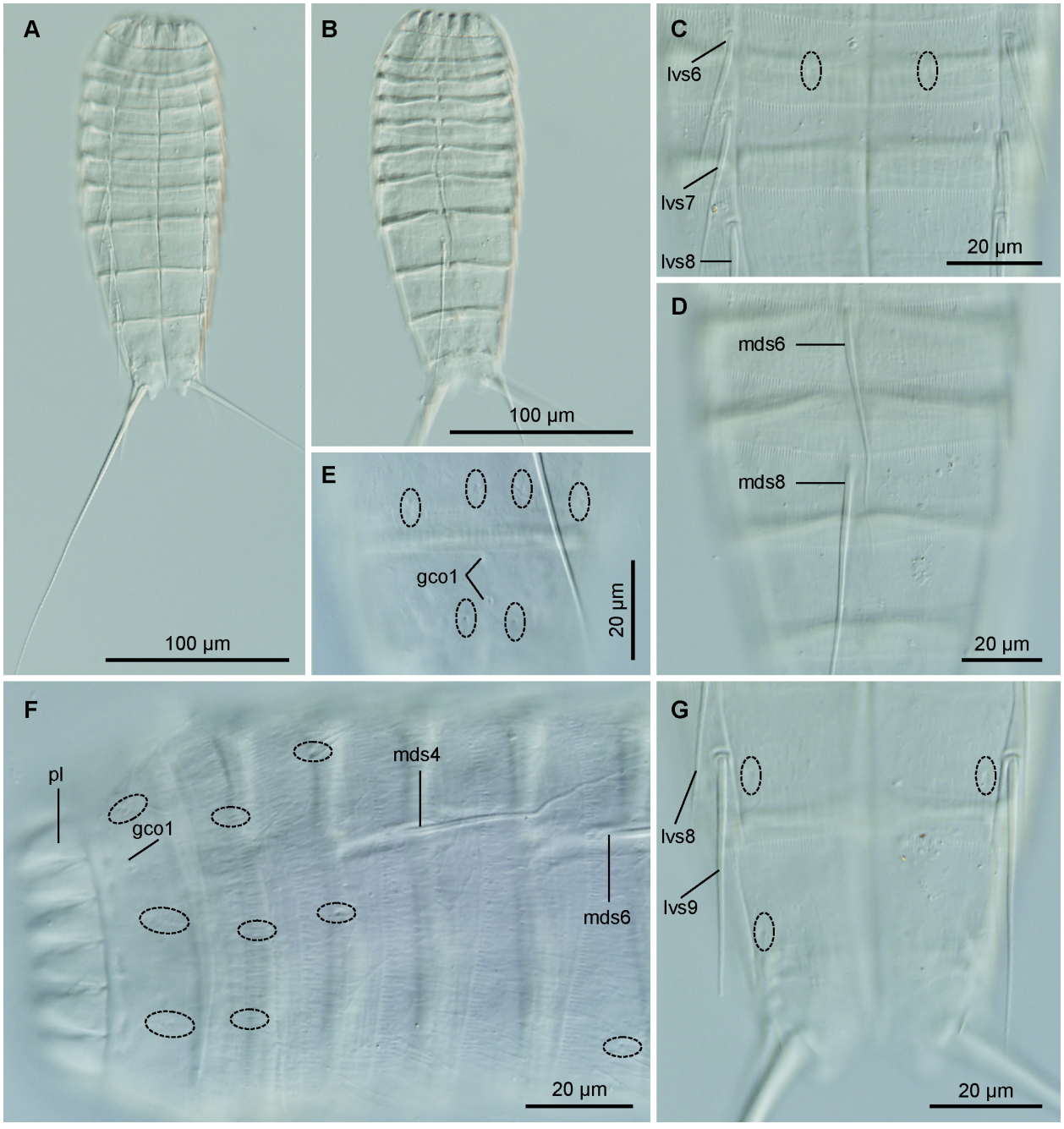
A
100 µm
B
100 µm
C
lvs6
lvs7
lvs8
20 µm
D
mds6
mds8
20 µm
E
gco1
20 µm
F
pl
gco1
mds4
mds6
20 µm
G
lvs8
lvs9
20 µm

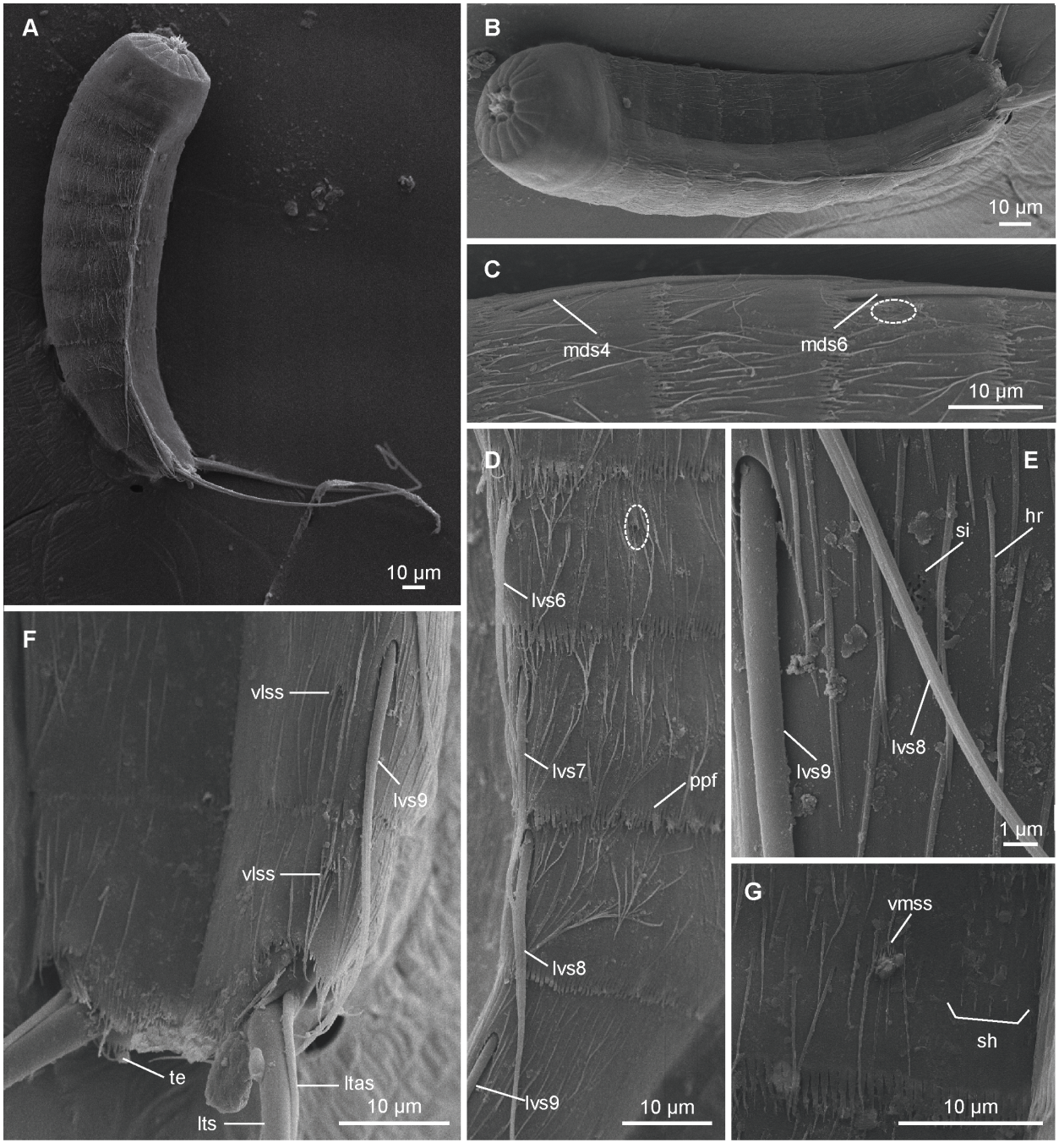
A
10 µm
B
10 µm
C
mds4
mds6
10 µm
D
lvs6
lvs7
ppf
lvs8
lvs9
10 µm
E
si
hr
lvs8
lvs9
1 µm
F
vlss
lvs9
vlss
te
ltas
lts
10 µm
G
vmss
sh
10 µm

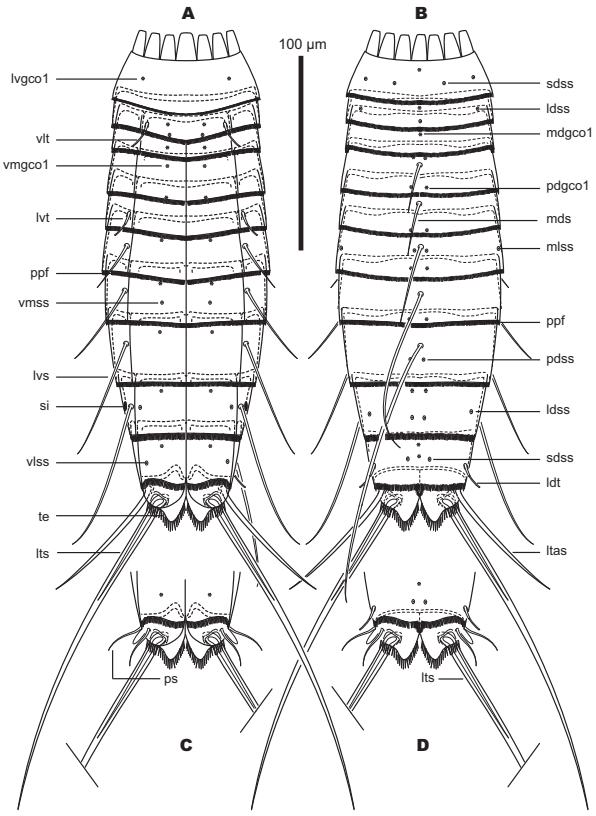

ACCEPTED MANUSCRIPT

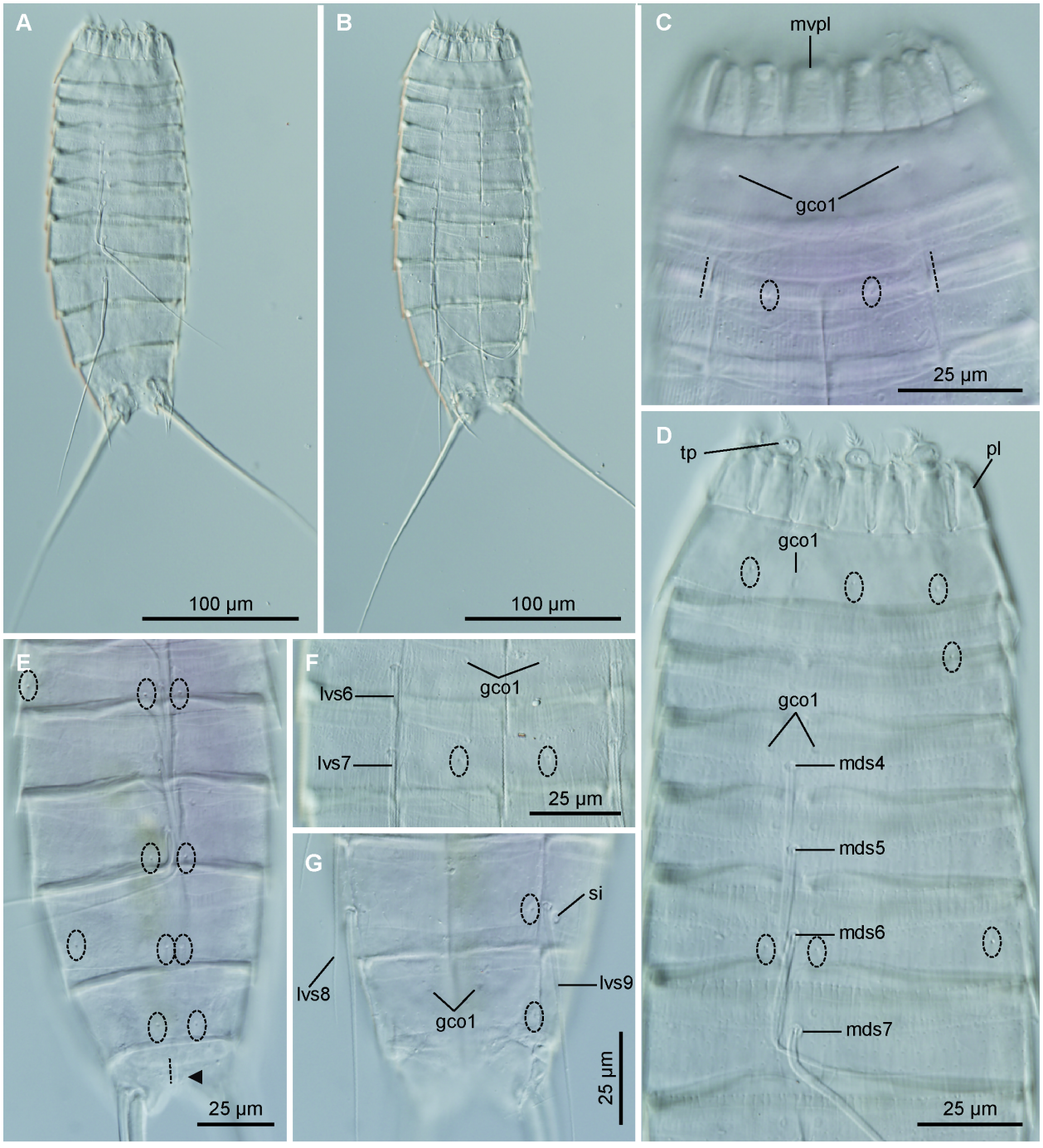
A
100 µm
B
100 µm
C
mvpl
gco1
25 µm
D
tp
pl
gco1
gco1
mds4
mds5
mds6
mds7
25 µm
E
25 µm
F
lvs6
gco1
lvs7
25 µm
G
si
lvs8
lvs9
gco1
25 µm

ACCEPTED MANUSCRIPT

The **Author** hereby grants the Journal Zoologischer Anzeiger full and exclusive rights to the manuscript, all revisions, and the full copyright. The Journal XXX rights include but are not limited to the following: (1) to reproduce, publish, sell, and distribute copies of the manuscript, selections of the manuscript, and translations and other derivative works based upon the manuscript, in print, audio-visual, electronic, or by any and all media now or hereafter known or devised; (2) to license reprints of the manuscript to third persons for educational photocopying; (3) to license others to create abstracts of the manuscript and to index the manuscript; (4) to license secondary publishers to reproduce the manuscript in print, microform, or any computer-readable form, including electronic on-line databases; and (5) to license the manuscript for document delivery. These exclusive rights run the full term of the copyright, and all renewals and extensions thereof. I hereby accept the terms of the above Author Agreement and I sign on behalf of the authors.

Nuria Sánchez

Date: 28/02/2019

ACCEPTED MANUSCRIPT